

The Limits of the Hubbard Model

DAVID GRABOVSKY

May 24, 2019

Contents

1	Introduction and Abstract	4
 I The Hubbard Hamiltonian		5
2	Preliminaries	6
3	Derivation of the Hubbard Model	9
3.1	Obtaining the Hamiltonian	9
3.2	Discussion: Energy Scales	10
4	Variants and Conventions	12
5	Symmetries of the Hubbard Model	14
5.1	Discrete Symmetries	14
5.2	Gauge Symmetries	14
5.3	Particle-Hole Symmetry	15
 II Interaction Limits		17
6	The Fermi-Hubbard Model	18
6.1	Single Site: Strong Interactions	18
6.2	Tight Binding: Weak Interactions	20
7	The Bose-Hubbard Model	22
7.1	Single Site: Strong Interactions	22
7.2	Tight Binding: Weak Interactions	24
 III Lattice Limits		25
8	Two Sites: Fermi-Hubbard	26
8.1	One Electron	26
8.2	Two Electrons	27
8.3	Three Electrons	28
8.4	Complete Solution	29
9	Two Sites: Bose-Hubbard	33
9.1	One and Two Bosons	33
9.2	Many Bosons	35
9.3	High-Temperature Limit	36
10	Conclusions and Outlook	38

IV Appendices	40
A The Hubbard Model from Many-Body Theory	41
B Some Algebraic Results	42
C Fermi-Hubbard Limits	43
C.1 No Hopping	43
C.2 No Interactions	44
D Bose-Hubbard Limits	44
D.1 No Hopping	44
D.2 No Interactions	46
E Two-Site Thermodynamics	47
E.1 Fermi-Hubbard Model	47
E.2 Bose-Hubbard Model	49
F Tridiagonal Matrices and Recurrences	50

1 Introduction and Abstract

The Hubbard model was originally written down in the 1960’s as an attempt to describe the behavior of electrons in a solid [1]. It envisions a lattice of stationary atoms, populated by electrons that can either be stuck to an atom or hop (tunnel) between neighboring atoms [12]. In some sense the Hubbard model is like a quantum egg carton, with prescribed rules about how eggs can occupy or shift lattice sites. The eggs are quantum-mechanical as well: they can sit on top of one another or exist in a delocalized superposition across all the wells, and they can have spin dictating how many of them are allowed on the same site. The system’s Hamiltonian consists of three terms—one favoring localization on lattice sites (hard-boiled eggs), another favoring delocalization across the lattice (raw eggs), and a third simply counting the number of particles. The competition between these behaviors lies at the heart of the Hubbard model [24], and the end result is a ground state somewhere between raw and hard-boiled: a sunny side up omelet.

The Hubbard model is the simplest Hamiltonian that incorporates both kinetic and potential energy contributions (hopping/tunneling and Coulomb-like interactions, respectively) [28]; it is also the simplest many-body Hamiltonian that cannot be reduced to a single-particle theory [4]. Despite this simplicity, the model has eluded an analytical solution (except in one dimension [8]) for over 50 years: even its ground state is unknown. Much is known about the model, however, and what we do know reveals incredibly rich behavior: Mott insulating phases, quantum magnetism, superfluidity, possible connections to high-temperature superconductivity, and more [28]. The prospect of high- T_c superconductivity hiding in the Hubbard model’s physics has spurred both theoretical and experimental research; in recent years, renewed interest has focused on the model’s realization in ultracold-atom experiments [14] [11] using optical lattice potentials to simulate the atomic lattice.

While the full Hubbard Hamiltonian remains unsolved, certain limiting cases of the model are both tractible and physically interesting [24]. This thesis explores a few of these limits in the hope of coming to a fuller understanding, or at least an appreciation, for what the model does by looking at its extremes. The organization of the thesis is as follows: In Part I, we introduce basic tools from quantum mechanics and statistical physics, derive the Hubbard Hamiltonian from a general two-body theory in second quantization, formalize our conventions and notation, and take a brief look at the Hubbard Hamiltonian’s deep symmetries. In Part II, we look at the limiting cases of no hopping (called the atomic limit [28]) and of no interactions (called the tight-binding limit [4]) for both the Fermi and Bose variants of the Hubbard Hamiltonian. In Part III, we restrict to a lattice of two sites, where we can exactly diagonalize the Hamiltonian and determine the system’s thermodynamic properties. Finally, Part IV contains the appendices, where we collect several important but technical computations.

Part I

The Hubbard Hamiltonian

Table of Contents

2 Preliminaries	6
3 Derivation of the Hubbard Model	9
3.1 Obtaining the Hamiltonian	9
3.2 Discussion: Energy Scales	10
4 Variants and Conventions	12
5 Symmetries of the Hubbard Model	14
5.1 Discrete Symmetries	14
5.2 Gauge Symmetries	14
5.3 Particle-Hole Symmetry	15

We begin our journey by collecting some crucial formalism and basic material from quantum and statistical mechanics: this includes the theory of periodic potentials, second-quantized notation for many-body quantum mechanics, and expectation values of quantum observables at finite temperature. Next, we will “derive” the Hubbard model by starting with an extremely general many-body theory that allows for arbitrary two-body interactions. Choosing a convenient lattice basis, we will make successively more severe approximations that constrain the theory to a form that eventually becomes the Fermi-Hubbard Hamiltonian.

With the setup out of the way, we’ll discuss the bosonic and fermionic variants of the model and establish a few important notational conventions. Finally, we will look at several different types of symmetries enjoyed by the Hubbard Hamiltonian. These include the geometrical symmetries of its lattice, the conservation of particle number and spin, and an important interchange transformation that generates a symmetry between particles and holes, or absences of particles. These symmetries will prove immensely helpful in achieving our main goal of analyzing the model’s limiting behaviors.

2 Preliminaries

Quantum Mechanics. We assume a firm grounding in the standard principles of quantum mechanics. To wit [23], the set of quantum states is a (rigged) Hilbert space \mathcal{H} of countable dimension, in which each state $|\psi\rangle$ is a unit vector (formally, a ray). Every observable \hat{A} is a self-adjoint operator on \mathcal{H} , its spectrum represents the set of possible measured values of \hat{A} , and its eigenbasis consists of states with a definite A -value. There is a distinguished observable \hat{H} called the Hamiltonian that represents a system's energy and generates time translations via the Schrödinger equation: $\hat{H}|\psi\rangle = i\hbar\frac{\partial}{\partial t}|\psi\rangle$. Similarly, the momentum operator generates translations in space, and the spin operator generates spatial rotations. An observable commutes with \hat{H} (resp. the generator of a symmetry parameterized by λ) iff it is conserved, i.e. constant in time (resp. constant with respect to λ). Iff two observables \hat{A} and \hat{B} commute (written $[A, B] = 0$), then they admit a common eigenbasis; moreover, \hat{A} is invariant under the symmetry generated by \hat{B} , and vice versa.

Periodic Potentials. In simple cases, the \hat{H} is the sum of kinetic and potential energy contributions. In the position basis, the momentum operator $\hat{\mathbf{p}}$ looks like $-i\hbar\nabla$, so

$$\hat{H} = \hat{T} + \hat{V} = \frac{\hat{\mathbf{p}}^2}{2m} + \hat{V}(\mathbf{r}) = -\frac{\hbar^2}{2m}\nabla^2 + \hat{V}(\mathbf{r}), \quad (2.1)$$

Since we will be interested in lattice models, consider the case where V is periodic. In one-dimensional systems with a lattice symmetry $V(x) = V(x + a)$, Bloch's theorem [3] states that stationary solutions to the Schrödinger equation, called Bloch states, are products of a plane wave and a periodic function u with the lattice's periodicity, $u(x) = u(x + a)$:

$$\hat{H}\phi(x) = E\phi(x) \implies \phi_q^{(n)}(x) = e^{iqx/\hbar}u_q^{(n)}(x). \quad (2.2)$$

Here q is the quasimomentum¹ labeling the plane wave. However, q does not uniquely identify the Bloch state because of the periodicity of $e^{iqx/\hbar}$, which confines the state's momentum to an interval: the first Bloch band. To reach higher energies and bands, introduce the band index n , which labels the branch of the energy as a function of q .

As suggested by the plane waves, Bloch states are spatially delocalized over the lattice but have definite momentum. Position and momentum in quantum mechanics are canonically dual through the Fourier transform, so we may also define maximally localized wavefunctions, called Wannier states [3]. Let our lattice have M sites labeled by j . Then the Wannier state localized at position $x = x_j$ is

$$w_j^{(n)}(x) = \frac{1}{\sqrt{M}} \sum_{q \in \Lambda^*} e^{-iqx_j/\hbar} \phi_q^{(n)}(x) \iff \phi_q^{(n)} = \frac{1}{\sqrt{M}} \sum_{j \in \Lambda} e^{iqx_j/\hbar} w_j^{(n)}(x). \quad (2.3)$$

Finally, the above generalizes to higher dimensions. Bloch states factor as products of ϕ 's in each direction V is periodic, and Wannier states factor as products of 1-dimensional w 's.

¹The prefix “quasi” indicates that q is a discrete version of the momentum p , suited to life on a lattice.

Many-Body Physics. The main features of many-body lattice systems are contained in the name: (1) they consist of multiple indistinguishable particles described by a wavefunction $\Psi(\mathbf{r}_1, \dots, \mathbf{r}_N)$ of their positions; and (2) these particles occupy and (3) move between lattice sites labeled by j at positions $\mathbf{r} = \mathbf{r}_j$.

(1) Indistinguishability means that interchanging two particles yields the same physical state up to a global phase θ , and that doing so twice returns the original state [7]:

$$\begin{aligned}\Psi(\mathbf{r}_i, \mathbf{r}_j) &= e^{i\theta} \Psi(\mathbf{r}_j, \mathbf{r}_i) = e^{2i\theta} \Psi(\mathbf{r}_i, \mathbf{r}_j) \implies \\ e^{2i\theta} &= 1 \implies e^{i\theta} = \pm 1.\end{aligned}\quad (2.4)$$

Thus the many-body wavefunction is either symmetric or antisymmetric under particle exchange: $\Psi(\mathbf{r}_i, \mathbf{r}_j) = \pm \Psi(\mathbf{r}_j, \mathbf{r}_i)$.² The plus sign is taken on by bosons, while the minus sign is taken on by fermions. Fermion antisymmetry leads to Pauli exclusion: if two fermions occupy the same state, exchanging them cannot affect the many-body wavefunction; but it also incurs a minus sign, so $\Psi = -\Psi \implies \Psi = 0$.

(2) Formally, many-body states are (anti)symmetrized tensor products of single-particle states; these states can be written in a more elegant form as Fock states [7]. Instead of answering the question “which particle is in which state?” with a suitably symmetrized tensor product, we can answer “how many particles are there in each state?” by labeling states $|\Psi\rangle = |n_1, n_2, \dots\rangle$, where n_α is the number of particles in single-particle state $|\alpha\rangle$. For fermions, $n_\alpha \in \{0, 1\}$, while for bosons, $n_\alpha \in \mathbb{N}$. The total occupation number is $N = \sum_\alpha n_\alpha$.

(3) The empty lattice $|0, 0, \dots\rangle = |0\rangle$ is called the vacuum state, and any state may be built from the vacuum by applying the creation and annihilation operators [21], defined by the canonical (anti)commutation relations:

$$[\hat{a}_\alpha, \hat{a}_\beta] = 0 = [\hat{a}_\alpha^\dagger, \hat{a}_\beta^\dagger]; \quad [\hat{a}_\alpha, \hat{a}_\beta^\dagger] = \delta_{\alpha\beta}, \quad (\text{bosons}) \quad (2.5)$$

$$\{\hat{c}_\alpha, \hat{c}_\beta\} = 0 = \{\hat{c}_\alpha^\dagger, \hat{c}_\beta^\dagger\} \quad \{\hat{c}_\alpha, \hat{c}_\beta^\dagger\} = \delta_{\alpha\beta}. \quad (\text{fermions}) \quad (2.6)$$

So \hat{a}_α^\dagger adds a boson to state $|\alpha\rangle$, while \hat{a}_α destroys a boson already in $|\alpha\rangle$: in general, $\hat{a}_\alpha^\dagger |n_\alpha\rangle = \sqrt{n_\alpha + 1} |n_\alpha + 1\rangle$ and $\hat{a}_\alpha |n_\alpha\rangle = \sqrt{n_\alpha} |n_\alpha - 1\rangle$. For fermions, the anticommutation relations imply that $(\hat{c}_\alpha^\dagger)^2 = 0$: creating two fermions in the same state is impossible. Thus Pauli exclusion proves that $n_\alpha \in \{0, 1\}$ for fermions, so we have $\hat{c}_\alpha^\dagger |0\rangle = |1_\alpha\rangle$ and $\hat{c}_\alpha |1_\alpha\rangle = |0\rangle$. Moreover, note that $\hat{a}_\alpha |0\rangle = \hat{c}_\alpha |0\rangle = 0$. As a result, the operators $\hat{n}_\alpha^B \equiv \hat{a}_\alpha^\dagger \hat{a}_\alpha$ and $\hat{n}_\alpha^F \equiv \hat{c}_\alpha^\dagger \hat{c}_\alpha$ are number operators that count the number of particles in state $|\alpha\rangle$, and provide a precise answer to the question second quantization was designed to answer.

As a very useful shorthand, we introduce the field operators [28], loosely defined as all possible ways to create or destroy the wavefunction $\psi_\alpha(x)$ representing state $|\alpha\rangle$:

$$\hat{\psi}_B^\dagger(\mathbf{r}) = \sum_\alpha \psi_\alpha^*(\mathbf{r}) \hat{a}_\alpha^\dagger; \quad \hat{\psi}_B(\mathbf{r}) = \sum_\alpha \psi_\alpha(\mathbf{r}) \hat{a}_\alpha, \quad (\text{bosons}) \quad (2.7)$$

$$\hat{\psi}_F^\dagger(\mathbf{r}) = \sum_\alpha \psi_\alpha^*(\mathbf{r}) \hat{c}_\alpha^\dagger; \quad \hat{\psi}_F(\mathbf{r}) = \sum_\alpha \psi_\alpha(\mathbf{r}) \hat{c}_\alpha. \quad (\text{fermions}) \quad (2.8)$$

²In 2-dimensional systems, this argument fails because of topological issues related to the paths the particles would need to take to actually be exchanged [6]. While $\theta = 0, \pi$ corresponds to bosons and fermions, respectively, particles taking on other values of θ are called (abelian) *anyons*.

This procedure promotes the wavefunctions to operators satisfying the algebra (2.5–2.6) and is therefore called second quantization. The same can be done with observables: the matrix elements of a (single-particle) operator \hat{A} become

$$A_{\alpha\beta} = \langle \alpha | \hat{A} | \beta \rangle = \int d^3r \psi_\alpha^*(\mathbf{r}) \hat{A}(\mathbf{r}) \psi_\beta(\mathbf{r}) \longrightarrow \int d^3r \hat{\psi}_\alpha^\dagger(\mathbf{r}) \hat{A}(\mathbf{r}) \hat{\psi}_\beta(\mathbf{r}). \quad (2.9)$$

Operators that couple multiple particles (i.e. interparticle interactions) come with as many d^3r integrals and copies of $\hat{\psi}^{(\dagger)}$ as particles they couple together.

Statistical Mechanics. Of the ingredients we will need from statistical mechanics, partition functions and expectation values are the most important. At temperature T , define the “coldness” $\beta \equiv 1/k_B T$, and recall the partition function $Z(\beta)$ [25], which describes how energy is partitioned among the system’s energy eigenstates $|\alpha\rangle$:

$$Z(\beta) \equiv \text{Tr}(e^{-\beta\hat{H}}) = \sum_{\alpha} \langle \alpha | e^{-\beta\hat{H}} | \alpha \rangle = \sum_{\alpha} e^{-\beta E_{\alpha}}. \quad (2.10)$$

Here E_{α} is the energy eigenvalue of $|\alpha\rangle$. The expectation value of any observable \hat{A} with eigenvalues λ_{α} at temperature T is normalized by Z :

$$\langle \hat{A} \rangle_{\beta} \equiv \frac{1}{Z} \text{Tr}(\hat{A} e^{-\beta\hat{H}}) = \frac{1}{Z} \sum_{\alpha} \langle \alpha | \hat{A} e^{-\beta\hat{H}} | \alpha \rangle = \frac{1}{Z} \sum_{\alpha} \lambda_{\alpha} e^{-\beta\hat{H}}. \quad (2.11)$$

We see that $\langle \hat{A} \rangle$ is a weighted sum of the possible outcomes its measurement can produce. The weight $e^{-E_{\alpha}/k_B T}$ is called the Boltzmann factor, and measures how likely λ_{α} is to occur by balancing the energy of $|\alpha\rangle$ ($\sim E_{\alpha}$) against the available energy ($\sim k_B T$) in the system.

Finally, a word on statistical ensembles [25]. When making claims about a system’s thermodynamics and the evolution of its statistical properties, we must specify which of its properties to hold constant. In the microcanonical (ENV) ensemble, the total energy, particle number, and volume are fixed: the system is enclosed in an insulating test tube. Meanwhile, in the grand canonical (μVT) ensemble, the chemical potential, volume, and temperature are held constant: the system is open and in contact with a reservoir of heat. There are other ensembles (notably grand canonical or NVT ensemble), but we will primarily use these two, especially the μVT .

3 Derivation of the Hubbard Model

We will start with a general many-body theory of fermions in a periodic lattice potential $V_{\text{lat}}(\mathbf{r})$, exposed to an additional trapping potential $V_{\text{tr}}(\mathbf{r})$. The lattice Λ can have any dimension d and any geometry, and consists of M sites labeled by j . In addition to the kinetic, lattice, and trapping terms, the many-body Hamiltonian contains a contact interaction that models Coulomb repulsion between electrons on the same site.

We will closely follow [28] for the majority of the derivation. In second quantization with $\sigma \in \{\uparrow, \downarrow\}$ labeling the spin of fermions, the full Hamiltonian $\hat{H} = \hat{H}_0 + \hat{H}_{\text{int}}$ reads

$$\begin{aligned}\hat{H}_0 &= \sum_{\sigma} \int d^3r \hat{\psi}_{\sigma}^{\dagger}(\mathbf{r}) \left[-\frac{\hbar^2}{2m} \nabla^2 + V_{\text{lat}}(\mathbf{r}) + V_{\text{tr}}(\mathbf{r}) \right] \hat{\psi}_{\sigma}(\mathbf{r}), \\ \hat{H}_{\text{int}} &= \frac{g}{2} \sum_{\sigma\sigma'} \int d^3r \hat{\psi}_{\sigma}^{\dagger}(\mathbf{r}) \hat{\psi}_{\sigma'}^{\dagger}(\mathbf{r}) \hat{\psi}_{\sigma'}(\mathbf{r}) \hat{\psi}_{\sigma}(\mathbf{r}), \quad g = 4\pi\hbar^2 a_s / m.\end{aligned}\quad (3.1)$$

In \hat{H}_0 , the first term is the kinetic energy of a single particle; the second term describes an optical lattice whose amplitude determines the probability of tunneling between neighboring sites; and the last term is typically a shallow quadratic potential in experiments [28]. The term \hat{H}_{int} is a general 2-body interaction with coupling constant proportional to the scattering length a_s , which is the radius of the hard sphere whose contact interactions roughly match the strength of the coupling at hand [16], and m the mass of the fermion.

3.1 Obtaining the Hamiltonian

The Hubbard model is derived from \hat{H} following three steps:

1. Choose Wannier functions as the basis of states and expand the field operators in terms of Wannier states. Then restrict to the first Bloch band: This makes the Hubbard model an effective low-energy theory, and excludes all couplings between bands [28].
2. Write \hat{H} in terms of the reduced field operators and massage it into a palatable form.
3. Further reduce to on-site (contact) interactions in \hat{H}_{int} and nearest-neighbor hopping in \hat{H}_0 , and move to the grand canonical ensemble to obtain the Hubbard Hamiltonian.

Step 1. As per the definition (2.8), $\hat{\psi}^{(\dagger)}$ should sum over all possible Wannier states, which are labeled by their Bloch band and lattice site. The field operators responsible for creating and destroying electrons of spin σ on the lattice are therefore

$$\hat{\psi}_{\sigma}^{\dagger} = \sum_{n,j} w_j^{*(n)}(\mathbf{r}) \hat{c}_{j\sigma}^{\dagger}; \quad \hat{\psi}_{\sigma} = \sum_{n,j} w_j^{(n)}(\mathbf{r}) \hat{c}_{j\sigma}. \quad (3.2)$$

Restricting to $n = 1$ constitutes the “single-band approximation,” and we henceforth remove the sum over n above and drop the band index on the Wannier states.

Step 2. Directly substituting $\hat{\psi}_\sigma^{(\dagger)} = \sum_j w_j^{(*)}(\mathbf{r}) \hat{c}_{j\sigma}^{(\dagger)}$ into (3.1), we obtain (see Appendix A)

$$\hat{H} = - \sum_{ij,\sigma} t_{ij} \hat{c}_{i\sigma}^\dagger \hat{c}_{j\sigma} + \frac{1}{2} \sum_{\sigma\sigma'} \sum_{ijkl} U_{ijkl} \hat{c}_{i\sigma}^\dagger \hat{c}_{j\sigma'}^\dagger \hat{c}_{k\sigma'} \hat{c}_{l\sigma} + \sum_{i,\sigma} \varepsilon_i \hat{n}_{i\sigma}, \quad (3.3)$$

where the tunneling matrix t_{ij} and interaction matrix U_{ijkl} are defined in Appendix A and further discussed below. The external trapping potential $\varepsilon_i \equiv V_{\text{tr}}(\mathbf{r}_i)$ is occasionally shallow enough for us to ignore differences in ε between lattice sites. We will soon choose to set $\varepsilon = 0$, although (as we will see below) this will not generally get rid of the \hat{n} term.

Step 3. We specialize (3.3) by dropping most of the couplings between lattice sites. Only contact terms $U \equiv 2U_{iiii}$ are kept, and we assume that t_{ij} is nonzero only when i and j are neighboring lattice sites, denoted by $\langle ij \rangle$ [4]. Finally, we will pass to the grand canonical ensemble (an open thermodynamic system) by making the transformation $\hat{H} \rightarrow \hat{H} - \mu \hat{N}$, where $\hat{N} = \sum_{i\sigma} \hat{n}_{i\sigma}$ is the total number operator. We therefore have

$$\hat{H} = - \sum_{\langle ij \rangle, \sigma} t_{ij} \hat{c}_{i\sigma}^\dagger \hat{c}_{j\sigma} + U \sum_{i,\sigma\sigma'} \hat{c}_{i\sigma}^\dagger \hat{c}_{i\sigma'}^\dagger \hat{c}_{i\sigma'} \hat{c}_{i\sigma} + \sum_{i,\sigma} (\varepsilon_i - \mu) \hat{n}_{i\sigma}. \quad (3.4)$$

Three more aesthetic changes are in order. First, we assume that all lattice sites have the same tunneling constant $t_{ij} = t_{ji} \equiv t$; to ensure the hermiticity of \hat{H} , we must add $\hat{c}_{j\sigma}^\dagger \hat{c}_{i\sigma}$ to the tunneling term. Second, in terms of number operators, the interaction term reads

$$\sum_{i,\sigma\sigma'} \hat{c}_{i\sigma}^\dagger \hat{c}_{i\sigma'}^\dagger \hat{c}_{i\sigma'} \hat{c}_{i\sigma} = \sum_{i,\sigma\sigma'} \hat{c}_{i\sigma}^\dagger \hat{n}_{i\sigma'} \hat{c}_{i\sigma} = \sum_{i,\sigma \neq \sigma'} \hat{n}_{i\sigma} \hat{n}_{i\sigma'} = \sum_i \hat{n}_{i\uparrow} \hat{n}_{i\downarrow}, \quad (3.5)$$

where we have used the commutation relations of \hat{n} with $\hat{c}^{(\dagger)}$ (See Appendix B) to reduce the sum to its usual form. And third, we will henceforth drop the trapping potential ε , in a sense trading it in for μ , which has the same physical effect on the model: there is no significant loss of generality. We therefore obtain the final form of the Hubbard Hamiltonian:

$$\hat{H} = -t \sum_{\langle ij \rangle, \sigma} (\hat{c}_{i\sigma}^\dagger \hat{c}_{j\sigma} + \hat{c}_{j\sigma}^\dagger \hat{c}_{i\sigma}) + U \sum_j (\hat{n}_{j\uparrow} \hat{n}_{j\downarrow}) - \mu \sum_{j,\sigma} \hat{n}_{j\sigma}. \quad (3.6)$$

3.2 Discussion: Energy Scales

Let's briefly take stock of what has happened so far. We started with a general many-body lattice Hamiltonian in an external trapping potential, with arbitrary two-body interactions. We expanded the field operators in the Wannier basis, restricted to the first Bloch band, and kept only contact interactions and nearest-neighbor hopping—this last approximation is called the tight binding limit [4] [3]. Finally, we homogenized the tunneling constant, dropped the trapping potential, and added a chemical potential to control the filling of the lattice. The resulting model (3.6) has three terms: $\hat{H} = -t \hat{H}_0 + U \hat{D} - \mu \hat{N}$.

\hat{H}_0 destroys a spin- σ particle on site i and creates one on site j (and vice versa); this “kinetic” term delocalizes electrons over the lattice to minimize kinetic energy, and has an eigenbasis of Bloch (momentum) states. \hat{D} models a screened Coulomb repulsion that assigns an energy cost to two electrons of opposite spin on the same site, and therefore counts double occupancy; minimizing this interaction energy favors localized electrons, and indeed \hat{D} is diagonal in the Wannier (position) basis. Finally, \hat{N} shifts the energy down according to the total number of electrons on the lattice; it will join \hat{D} in favoring localization. This competition between kinetic and interaction energies—between momentum and position—is fundamentally what gives the Hubbard model its rich behavior [28].

Before analyzing various limits of the model, we can say a few things about the constants U and t in special cases [28]. In Appendix A, $U \equiv 2U_{iiii}$ is defined by

$$U_{ijkl} \equiv g \int d^3r w_i^* w_j^* w_k w_l \implies U = 2g \int d^3r |w_i(\mathbf{r})|^4 = \frac{8\pi\hbar^2 a_s}{m} \int d^3r |w_i(\mathbf{r})|^4. \quad (3.7)$$

In very deep, cubically symmetric lattices, $V_{\text{lat}}(\mathbf{r}) \sim |\mathbf{r}|^2$ can be approximated by a paraboloid, in which case $w_i(\mathbf{r}) \sim e^{-s|\mathbf{r}|^2/2}$ is roughly Gaussian, with $s \in \mathbb{R}_+$ a dimensionless parameter describing the potential well’s depth. Then the interaction energy scales as

$$U \sim \frac{a_s}{m} \left(\int_{-\infty}^{\infty} dr |e^{-sr^2/2}|^4 \right)^3 \sim \frac{a_s}{ms^{3/2}}. \quad (3.8)$$

The tunneling energy, on the other hand, can be written in terms of the Bloch states (see Appendix A) and expressed in terms their quasimomentum \mathbf{q} through a dispersion relation $\varepsilon_{\mathbf{q}}$ [3], which can then be isolated and solved for:

$$t_{ij} = -\frac{1}{N} \sum_{\mathbf{q}} \varepsilon_{\mathbf{q}} e^{i\mathbf{q} \cdot (\mathbf{r}_i - \mathbf{r}_j)} \iff \varepsilon_{\mathbf{q}} = \sum_{ij} t_{ij} e^{-i\mathbf{q} \cdot (\mathbf{r}_i - \mathbf{r}_j)}. \quad (3.9)$$

In the tight binding limit, only nearest neighbors in the sum above survive. Define the lattice vector $\mathbf{a}_{ij} \equiv \mathbf{r}_i - \mathbf{r}_j$ and perform the sum over $\langle ij \rangle$ by arguing that each site i it has two nearest neighbors at $\mathbf{r}_i \pm \mathbf{a}_{ij}$ in each “direction” away from i , parameterized by j :

$$\varepsilon_{\mathbf{q}} = \sum_{\langle ij \rangle} t_{ij} e^{-i\mathbf{q} \cdot (\mathbf{r}_i - \mathbf{r}_j)} \longrightarrow t \sum_j \left[e^{-i\mathbf{q} \cdot \mathbf{a}_{ij}} + e^{i\mathbf{q} \cdot \mathbf{a}_{ij}} \right] = -2t \sum_j \cos(\mathbf{q} \cdot \mathbf{a}_{ij}). \quad (3.10)$$

For example, on a square lattice with lattice vectors $a_x \hat{\mathbf{x}}$ and $a_y \hat{\mathbf{y}}$, the dispersion relation would be $\varepsilon_{\mathbf{q}} = -2t (\cos(q_x a_x) + \cos(q_y a_y))$. Admittedly the notation above is sloppy, but we have traded generality and precision in describing the geometry of Λ for what hopefully amounts to a clearer physical picture. We will hereafter omit the sum over j , letting the symbol $\varepsilon_{\mathbf{q}}$ convey the instruction “project the quasimomentum onto each lattice vector, add up the cosines of the projections, and scale by $-2t$.” Physically, this relation describes the wavelike behavior of the eigenstates of the tight-binding Hamiltonian [3]; more philosophically, $\varepsilon_{\mathbf{q}}$ describes the degree to which spatial modes are delocalized, and consequently how well they “come together” in momentum space.

4 Variants and Conventions

The Hubbard model can be formulated for bosons as well as for fermions; the derivation for bosons follows the same lines as the one above. The two Hamiltonians are almost identical:

$$\hat{H}_F = -t \sum_{\langle ij \rangle, \sigma} (\hat{c}_{i\sigma}^\dagger \hat{c}_{j\sigma} + \hat{c}_{j\sigma}^\dagger \hat{c}_{i\sigma}) + U \sum_j (\hat{n}_{j\uparrow} \hat{n}_{j\downarrow}) - \mu \sum_{j,\sigma} \hat{n}_{j\sigma}; \quad (4.1)$$

$$\hat{H}_B = -t \sum_{\langle ij \rangle} (\hat{a}_i^\dagger \hat{a}_j + \hat{a}_j^\dagger \hat{a}_i) + \frac{U}{2} \sum_j \hat{n}_j (\hat{n}_j - 1) - \mu \sum_j \hat{n}_j. \quad (4.2)$$

The only difference, besides the statistics of the creation and annihilation operators, is that for bosons there are $\frac{1}{2}n(n-1)$ interacting pairs of particles: this accounts for the form of the U term [28]. Moreover, both of these Hamiltonians are grand-canonical; to move to the microcanonical ensemble, simply remove the μ terms from each one [25].

Below is a list standardizing the notation and conventions we will use from here on out (some differing slightly from usage above), intended primarily as a useful reference.

Λ, Λ^*	spatial lattice and its momentum dual
i, j	site indices labeling positions in Λ
k, l	quasimomentum indices labeling Λ^*
$\langle ij \rangle$	sites i and j are nearest neighbors
σ, σ'	spin indices for fermions, $\sigma \in \{\uparrow, \downarrow\}$
M	number of lattice sites, $M = \Lambda $
N	number of particles on the lattice
d	number of doubly occupied sites
$\mathbf{r}_j, \mathbf{a}_{ij}$	position of j in \mathbb{R}^3 ; lattice vector $\mathbf{r}_i - \mathbf{r}_j$
$\mathbf{q}_k, \varepsilon_k$	quasimomentum of k in \mathbb{R}^3 ; dispersion
$\hat{\psi}_{(\sigma)}^{(\dagger)}(\mathbf{r})$	field creation (destruction) operator
$w_j(\mathbf{r})$	Wannier state localized at j ($\mathbf{r} = \mathbf{r}_j$)
$\phi_k(\mathbf{r})$	Bloch state of momentum k ($\mathbf{q} = \mathbf{q}_k$)
$ \alpha\rangle, A_\alpha$	single-particle state; its \hat{A} -eigenvalue
$\hat{a}_j^\dagger / \hat{a}_j$	creates/destroys a boson on site $j \in \Lambda$
$\hat{c}_{j\sigma}^\dagger / \hat{c}_{j\sigma}$	creates/destroys a spin- σ fermion at j
$\hat{n}_{j(\sigma)}$	number operator at j (with spin σ)
\hat{H}_0, t	tunneling operator; hopping energy
\hat{D}, U	double occupancy operator; interactions
\hat{N}, μ	number operator; chemical potential
T, β	temperature and coldness, $\beta = 1/T$

Some more conventions follow. First, we will work in natural units $\hbar = k_B = 1$. Typically, $\mu > 0$ and $U > 0$, corresponding to nonzero lattice filling and repulsive interactions. Both $\mu < 0$ (preference against filling) and $U < 0$ (attractive interactions) are possible, however, and when we discuss the Bose-Hubbard model some problems with attractive interactions will be presented. Some of the results to come will depend on the dimensionless ratio μ/U , in which case only their relative sign will matter. On the other hand, since t directly controls the probability of tunneling between lattice sites, usually $t > 0$.

When labeling fermion states by their spin, $|\downarrow\rangle$ will precede $|\uparrow\rangle$. This choice is arbitrary but standard in the literature [8], and hints at a lifting of the degeneracy between $|\downarrow\rangle$ and $|\uparrow\rangle$ whereby spin-up states acquire more energy while spin-down states lose energy. When two spins occupy a single site, we will often denote the state $|\uparrow\downarrow\rangle$ by $|2\rangle$, and an empty site by $|0\rangle$.

Also, we will formally distinguish between *vectors* and their *labels*. Lattice sites in Λ are labeled by j , but have real-space positions \mathbf{r}_j ; likewise, quasimomenta \mathbf{q}_k will be labeled by $k \in \Lambda^*$. In this notation, we will often denote dot products $\mathbf{q}_k \cdot \mathbf{r}_j$ simply by jk , and $\mathbf{q}_k \cdot \mathbf{a}_{ij}$ will sometimes be shortened to ka when the meaning is clear.

5 Symmetries of the Hubbard Model

The Hubbard model enjoys many rich and surprising symmetries, some of which we briefly discuss in this section. Throughout, our main example will be the one-dimensional Fermi-Hubbard model of M sites with periodic boundary conditions: in fact, thanks to its symmetries this model has been exactly solved using the celebrated Bethe ansatz. The excellent review [8], as well as many other monographs, have been devoted to studying the algebraic properties of Hubbard-like Hamiltonians; from this literature we can give only the briefest taste of the physics hidden in these symmetries.

5.1 Discrete Symmetries

The geometry of the Hubbard lattice Λ embodies certain discrete symmetries. For instance, the 1D periodic M -site lattice is a regular M -gon, and thus has dihedral symmetry group D_{2M} , including lattice rotations $\mathbb{Z}/M\mathbb{Z}$ and lattice “flips” $\mathbb{Z}/2\mathbb{Z}$. As another example, an infinite square lattice in 2 dimensions has symmetry group \mathbb{Z}^2 ; this includes translations in x and y , rotations by $\pi/2$, and x/y flips. More complicated lattices, such as triangular or honeycomb lattices, have more complicated symmetries.

To pass from symmetries of Λ to symmetries of the Hubbard model, we must (1) construct operators out of $\hat{c}_{j\sigma}^\dagger$ and $\hat{c}_{j\sigma}$ that effect the symmetry transformations; (2) prove that these operators generate a unitary representation of the associated symmetry group; and (3) show that the Hubbard Hamiltonian is invariant under the action of these operators [23]. It turns out that \hat{H} inherits all of the symmetries of Λ : we will not prove this rigorously here, but see [8] for the elegant (if involved) example of $\mathbb{Z}/M\mathbb{Z}$ in 1 dimension. Physically, we can justify it by noting that $\hat{H} = -t\hat{H}_0 + U\hat{D} - \mu\hat{N}$ contains terms that affect only a single site or two neighboring sites. We should therefore expect that any (reasonable) transformation of Λ that preserves nearest neighbors should also be a symmetry of \hat{H} . If we set $t = 0$, then no two sites are correlated, and the entire symmetric group S_Λ of order $M!$, generated by permutations of sites, is respected by \hat{H} : this causes the $M!$ -fold degeneracy of each state.

Beyond the geometry of Λ , the Fermi-Hubbard model enjoys a spin-flip symmetry $\mathbb{Z}/2\mathbb{Z}$ generated by swapping all spins on the lattice. It is easy to see that \hat{H}_F is symmetric with respect to σ , so flipping all spins leaves \hat{H} unchanged.

5.2 Gauge Symmetries

Following the “Noether philosophy” that continuous symmetries correspond to conserved quantities, we are led to look for operators that commute with \hat{H} , as these will generate additional symmetries of the model. For instance, we might surmise that the number operator \hat{N} commutes with \hat{H} , since particle number is indeed conserved (see Appendix B for a proof). The conservation of particle number corresponds to a symmetry generated by transforming all of the creation operators by an overall phase. As a pleasant side effect, the global phase also leaves the tunneling term, and thus the entire Hamiltonian, invariant:

$$\begin{cases} \hat{c}_{j\sigma} \rightarrow e^{i\theta} \hat{c}_{j\sigma}, \\ \hat{c}_{j\sigma}^\dagger \rightarrow e^{-i\theta} \hat{c}_{j\sigma}^\dagger \end{cases} \implies \begin{cases} \hat{n}_{j\sigma} \rightarrow \hat{n}_{j\sigma} \\ \hat{H}_0 \rightarrow \hat{H}_0 \end{cases} \implies \hat{H} \rightarrow \hat{H}. \quad (5.1)$$

Since the generator θ of the symmetry is periodic, \hat{H} has a global $U(1)$ gauge symmetry.

More interestingly, the Fermi-Hubbard Hamiltonian commutes with the “spin” operators, defined analogously to particle number and with the help of the Pauli matrices σ_i [17]:

$$\hat{N} = \sum_{j \in \Lambda} (\hat{n}_{j\uparrow} + \hat{n}_{j\downarrow}), \quad \hat{S}_i = \frac{1}{2} \sum_{j, \sigma, \sigma'} \hat{c}_{j\sigma}^\dagger \sigma_i \hat{c}_{j\sigma'} \implies \hat{S}_z = \frac{1}{2} \sum_j (\hat{n}_{j\uparrow} - \hat{n}_{j\downarrow}) \quad (5.2)$$

Indeed, the \hat{S}_i generate a representation of $SU(2)$ and thus describe spin, and \hat{H} commutes with all of them, making it rotationally invariant (see Appendix B).

5.3 Particle-Hole Symmetry

One final symmetry of the Fermi-Hubbard model treats particles and “holes,” or absences of particles, on equal footing. The dynamics of a spin-up electron on a lattice site, for example, is completely equivalent to that of a spin-down hole, i.e. the absence of a single spin-down electron. To implement this symmetry, we need to interchange the roles of the creation and destruction operators [17]. On a 1D lattice Λ with M sites, define the Fermi operators

$$\hat{d}_{j\sigma}^\dagger = (-1)^j \hat{c}_{j\sigma}; \quad \hat{d}_{j\sigma} = (-1)^j \hat{c}_{j\sigma}^\dagger, \quad j \in \{1, \dots, M\} = \Lambda. \quad (5.3)$$

These new operators preserve the Hamiltonian. The kinetic term is entirely unchanged:

$$\begin{aligned} \hat{H}_0(\hat{d}) &= \sum_{\langle ij \rangle, \sigma} \left(\hat{d}_{i\sigma}^\dagger \hat{d}_{j\sigma} + \hat{d}_{j\sigma}^\dagger \hat{d}_{i\sigma} \right) = \sum_{\langle ij \rangle, \sigma} (-1)^{i+j} \left(\hat{c}_{i\sigma} \hat{c}_{j\sigma}^\dagger + \hat{c}_{j\sigma} \hat{c}_{i\sigma}^\dagger \right) = \\ &= \sum_{\langle ij \rangle, \sigma} (-1)^{i+j+1} \left(\hat{c}_{j\sigma}^\dagger \hat{c}_{i\sigma} + \hat{c}_{i\sigma}^\dagger \hat{c}_{j\sigma} \right) = \sum_{\langle ij \rangle, \sigma} \left(\hat{c}_{i\sigma}^\dagger \hat{c}_{j\sigma} + \hat{c}_{j\sigma}^\dagger \hat{c}_{i\sigma} \right) = \hat{H}_0(\hat{c}). \end{aligned} \quad (5.4)$$

In the third equality we have commuted the \hat{c} ’s past each other at the cost of a minus sign; then, since i, j are nearest neighbors on a 1D lattice, $i = j \pm 1$ implies that $i + j + 1$ is even and hence $(-1)^{i+j+1} = +1$. Meanwhile, the number operator is turned upside down:

$$\hat{n}_{j\sigma}(\hat{d}) = \hat{d}_{j\sigma}^\dagger \hat{d}_{j\sigma} = (-1)^{2j} \hat{c}_{j\sigma} \hat{c}_{j\sigma}^\dagger = 1 - \hat{c}_{j\sigma}^\dagger \hat{c}_{j\sigma} = 1 - \hat{n}_{j\sigma}(\hat{c}). \quad (5.5)$$

That is, the Fermi occupation numbers $n_{j\sigma} \in \{0, 1\}$ are interchanged under $\hat{c} \rightarrow \hat{d}$. This, in turn causes the double occupancy and total number operators to transform as

$$\hat{N}(\hat{d}) = \sum_{j, \sigma} \hat{n}_{j\sigma}(\hat{d}) = \sum_{j, \sigma} (1 - \hat{n}_{j\sigma}(\hat{c})) = N - \hat{N}(\hat{c}); \quad (5.6)$$

$$\begin{aligned}\hat{D}(\hat{d}) &= \sum_j \left(\hat{n}_{j\uparrow}(\hat{d}) \hat{n}_{j\downarrow}(\hat{d}) \right) = \sum_j (1 - \hat{n}_{j\uparrow}(\hat{c})) (1 - \hat{n}_{j\downarrow}(\hat{c})) = \\ &= \sum_j \left[1 + \hat{n}_{j\uparrow}(\hat{c}) \hat{n}_{j\downarrow}(\hat{c}) - \hat{n}_{j\uparrow}(\hat{c}) - \hat{n}_{j\downarrow}(\hat{c}) \right] = M + \hat{D}(\hat{c}) - \hat{N}(\hat{c}),\end{aligned}\quad (5.7)$$

where as usual N is the total particle number and $M = |\Lambda|$ is the number of lattice sites. The overall effect of these transformations on the Hubbard Hamiltonian is

$$\begin{aligned}\hat{H}(\hat{d}) &= -t\hat{H}_0(\hat{d}) + U\hat{D}(\hat{d}) - \mu\hat{N}(\hat{d}) = \\ &= -t\hat{H}_0(\hat{c}) + U(M + \hat{D}(\hat{c}) - \hat{N}(\hat{c})) - \mu(N - \hat{N}(\hat{c})) = \\ &= \hat{H}(\hat{c}) - (U - \mu)\hat{N}(\hat{c}) + (UM - \mu N).\end{aligned}\quad (5.8)$$

The last term is a constant shift in energy and can be discarded; the second term amounts to a shift in the chemical potential by U , and does not change the physics. In any case, we see that the particle-hole transformation (PHT) gives rise to a symmetry of the Hubbard model. This can be generalized to higher-dimensional geometries using the notion of a bipartite lattice [24], but the 1D model provides a convenient and instructive example. Notably, this transformation is not a symmetry of the Bose-Hubbard model, since it relies crucially on the anticommutation relations of the \hat{c} 's.

Let us briefly summarize all of the symmetries we have discussed. The geometrical symmetries $\text{Sym}(\Lambda)$ of the lattice form a group of spatial transformations under which \hat{H} is invariant. The Fermi-Hubbard model also has the spin-flip symmetry group $\mathbb{Z}/2\mathbb{Z}$. Both the Fermi and Bose variants of \hat{H} respect a global $U(1)$ gauge symmetry, associated to a global phase, from particle number conservation. They also enjoy rotational invariance, i.e. are invariant under a copy of $SU(2)$ generated by the spin operators \hat{S}_i . Finally, the Fermi-Hubbard model is invariant under the PHT described above. It turns out [8] that on a 1D lattice with an even number of sites, the Fermi-Hubbard model at half-filling has a “hidden” $SU(2)$ symmetry due to the PHT; away from half-filling, the full $SU(2) \times SU(2)$ symmetry decays to $[SU(2) \times SU(2)]/(\mathbb{Z}/2\mathbb{Z}) = SO(4)$. It is this miraculous symmetry, and the infinite set of invariants that the model affords, that eventually allowed for the exact solution of the Fermi-Hubbard model in 1 dimension by the celebrated Bethe ansatz.

Part II

Interaction Limits

Table of Contents

6	The Fermi-Hubbard Model	18
6.1	Single Site: Strong Interactions	18
6.2	Tight Binding: Weak Interactions	20
7	The Bose-Hubbard Model	22
7.1	Single Site: Strong Interactions	22
7.2	Tight Binding: Weak Interactions	24

Although the Hubbard model is unsolved in general, it can be diagonalized in the extreme limits of no tunneling ($t = 0$) and no interactions ($U = 0$). When we eliminate hopping, each lattice site becomes independent of the others, so it suffices to consider a single site, and a Wannier-like basis will naturally appear. When we eliminate the contact repulsion, we enter the *tight binding* regime, so named for the absence of repulsion, despite the fact that it is characterized by pure hopping between sites. It exhibits no spatial localization, and in a Bloch-like basis it decouples into independent momentum modes [24].

Over the next two sections, we will analyze these limits for the Fermi and Bose variants of the Hubbard model. Our systematic approach will be to (1) write down the Hamiltonian and find a suitable basis for its Hilbert space to work with; (2) diagonalize the Hamiltonian and discuss its ground state; and (3) work out the statistical mechanics of the system, computing the partition function, average (grand-canonical) energy $E = \langle \hat{H} + \mu \hat{N} \rangle = -t\langle \hat{H}_0 \rangle + U\langle \hat{D} \rangle$, and average occupation number $N = \langle \hat{N} \rangle$ at finite temperature.

6 The Fermi-Hubbard Model

6.1 Single Site: Strong Interactions

The Hamiltonian. At $t = 0$, the Fermi-Hubbard Hamiltonian is

$$\hat{H} = U \sum_j (\hat{n}_{j\uparrow} \hat{n}_{j\downarrow}) - \mu \sum_{j,\sigma} \hat{n}_{j\sigma} = \sum_j \hat{H}_j, \quad (6.1)$$

where $\hat{H}_j = U(\hat{n}_{j\uparrow} \hat{n}_{j\downarrow}) - \mu(\hat{n}_{j\uparrow} + \hat{n}_{j\downarrow})$ is the Hamiltonian for site j . This decoupling suggests that it suffices to solve the one-site model [24]; the eigenstates of (6.1) will be products of the single-site eigenstates. A single site may be empty, or occupied by one or two electrons: the Hilbert space is thus spanned by four states, with basis $\beta_j = \{|0\rangle_j, |\downarrow\rangle_j, |\uparrow\rangle_j, |2\rangle_j\}$, where $|2\rangle$ is the doubly occupied site. Since we have two fermions in a potential well, for deep lattices we may expect similarities to the results of [5], which studied the two-body problem in a harmonic trap. In any case, we see that \hat{H}_j acts diagonally on β_j :

$$\hat{H}_j |0\rangle = 0; \quad \hat{H}_j |\downarrow\rangle = -\mu |\downarrow\rangle; \quad \hat{H}_j |\uparrow\rangle = -\mu |\uparrow\rangle; \quad \hat{H}_j |2\rangle = (U - 2\mu) |2\rangle. \quad (6.2)$$

Therefore in this basis, the Hamiltonian takes the form $\hat{H}_j = \text{diag}(0, -\mu, -\mu, U - 2\mu)$.

Eigenstates and energies. The eigenstates of \hat{H}_j are the states of β_j , and the corresponding energies are above. The table below shows the ground state in every possible scenario:

Sign of μ	Sign of U	Size of μ/U	Ground state
$\mu > 0$	$U > 0$	$ \mu/U < 1$	$ \downarrow\rangle$ and $ \uparrow\rangle$
$\mu > 0$	$U > 0$	$ \mu/U > 1$	$ 2\rangle$
$\mu > 0$	$U < 0$	N/A	$ 2\rangle$
$\mu < 0$	$U > 0$	N/A	$ 0\rangle$
$\mu < 0$	$U < 0$	$ \mu/U < \frac{1}{2}$	$ 2\rangle$
$\mu < 0$	$U < 0$	$ \mu/U > \frac{1}{2}$	$ 0\rangle$

Table 1: Ground states of the single-site Fermi-Hubbard model.

Interestingly, when U and μ have opposite signs, their relative strengths are irrelevant for determining the ground state. Also, positive filling and strong repulsion ($U > \mu > 0$) favors a singly occupied site, but is ambivalent about its spin, producing a ground state degeneracy.

Full diagonalization. Having analyzed a single site, let us formally diagonalize (6.1). Our basis β will be the Fock states $\{|\boldsymbol{\sigma}\rangle\}$, where $\boldsymbol{\sigma} = (\sigma_1, \dots, \sigma_M)$ runs over all of the lattice sites in Λ , and each entry takes values in the single-site space, $\sigma_j \in \{0, \downarrow, \uparrow, 2\}$. Then (formally, by the properties of the tensor product) each site- j operator in \hat{H} acts “independently” on $|\boldsymbol{\sigma}\rangle$, either killing or scaling the entire Fock state according what is happening on site j . Therefore the full Hamiltonian acts diagonally on β :

$$\hat{H} |\boldsymbol{\sigma}\rangle = (U \hat{D} - \mu \hat{N}) |\boldsymbol{\sigma}\rangle = (U d - \mu N) |\boldsymbol{\sigma}\rangle \equiv E |\boldsymbol{\sigma}\rangle, \quad (6.3)$$

where d is the number of doubly occupied sites, and N is the total number of electrons on the lattice. (Then also $s \equiv N - 2d$ is the number of singly occupied sites.) Due to the geometrical symmetries of Λ , the ground state depends only on the number of (doubly) occupied lattice sites and hence on the ratio μ/U , and is invariant under lattice site permutations [8]. For example, the ground state of the repulsive model $U > \mu > 0$ fills each lattice site with a single electron of random spin; this situation is known as half-filling [24].

Statistical mechanics. The exact expressions for the partition function Z , average energy E , and average occupation N are unfortunately unenlightening and are therefore relegated to Appendix D; nevertheless, the plots of E and N shown below reveal interesting behavior.

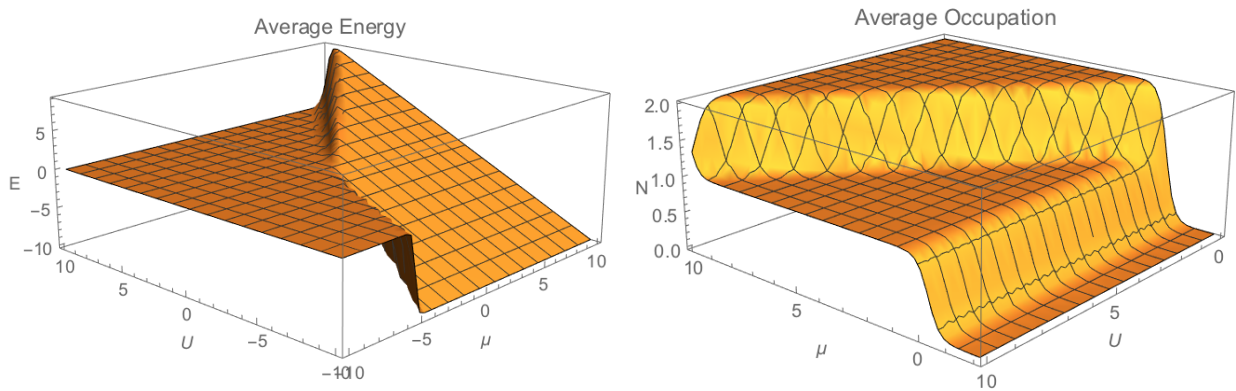


Figure 1: Average energy and density in the single-site Fermi-Hubbard model at $\beta = 5$.

In the energy graph, note the sharp ridges along $\mu = U$ (for $\mu, U > 0$) and $\mu = U/2$ (for $\mu, U < 0$). These ridges bound regions of the graph with distinct ground states—compare the possibilities listed in Table 6.1. In the graph of N , we may fix U and allow μ to rise: after the site fills with one electron, N plateaus until μ jumps by U , giving the system enough energy to doubly occupy the site. This feature is called the Mott gap [28], and makes the Hubbard model a Mott insulator, where the metal-insulator transition is due to electronic interactions instead of conventional band theory [3]. We can understand the Mott gap more viscerally by recalling that μ is the rate of change in the system’s energy in response to changes in particle number: $\mu = \frac{\partial E}{\partial N}$. As N rises from 1 to 2, μ jumps suddenly; so too must the system’s energy. Indeed, such a jump in energy is the hallmark of an insulating gap, and we can see its manifestation in the ridges of the energy graph above.

While not shown above, changing β washes out or sharpens the features discussed above. At absolute zero, the ridges and jumps above drop off as step functions, and the system is simply unable to accept a second electron until μ adds enough energy to overcome the Mott plateau. Positive temperature bathes the system in thermal energy, and in so doing smooths out any quantum-mechanical features [24]. This is fundamentally why low-temperature experiments, including realizations of the Fermi-Hubbard model in the lab [14], are so important. We will later turn to the question of whether and how quantum fluctuations, such as those induced by hopping terms, also wash out Mott-insulating behavior.

6.2 Tight Binding: Weak Interactions

The Hamiltonian. At $U = 0$, the Fermi-Hubbard Hamiltonian is

$$\hat{H} = -t \sum_{\langle ij \rangle, \sigma} (\hat{c}_{i\sigma}^\dagger \hat{c}_{j\sigma} + \hat{c}_{j\sigma}^\dagger \hat{c}_{i\sigma}) - \mu \sum_{j,\sigma} \hat{n}_{j\sigma} = \hat{H}_\uparrow + \hat{H}_\downarrow, \quad (6.4)$$

where \hat{H}_σ is the Hamiltonian for spin σ . We could try to isolate and solve the single-spin Hamiltonian, but it turns out to be more useful to decompose (6.4) in momentum space. In this section, we will follow [24] and [8], generalizing the latter to arbitrary lattices.

Momentum space operators. We define the momentum-space creation and annihilation operators by taking discrete Fourier transforms of their position-space counterparts:

$$\hat{c}_{k\sigma}^\dagger \equiv \frac{1}{\sqrt{M}} \sum_{j \in \Lambda} e^{i\mathbf{q}_k \cdot \mathbf{r}_j} \hat{c}_{j\sigma}^\dagger; \quad \hat{c}_{k\sigma} \equiv \frac{1}{\sqrt{M}} \sum_{j \in \Lambda} e^{-i\mathbf{q}_k \cdot \mathbf{r}_j} \hat{c}_{j\sigma}. \quad (6.5)$$

These mode expansions can be inverted to write $\hat{c}_{j\sigma}^{(\dagger)}$ in terms of $\hat{c}_{k\sigma}^{(\dagger)}$:

$$\hat{c}_{j\sigma}^\dagger \equiv \frac{1}{\sqrt{M}} \sum_{k \in \Lambda^*} e^{-i\mathbf{q}_k \cdot \mathbf{r}_j} \hat{c}_{k\sigma}^\dagger; \quad \hat{c}_{j\sigma} \equiv \frac{1}{\sqrt{M}} \sum_{k \in \Lambda^*} e^{i\mathbf{q}_k \cdot \mathbf{r}_j} \hat{c}_{k\sigma}. \quad (6.6)$$

Next, we substitute these expansions into \hat{H} . After some algebra (see Appendix C), we are left with a startlingly simple expression:

$$\hat{H} = -t \hat{H}_0 - \mu \hat{N} = \sum_{k,\sigma} (\varepsilon_k - \mu) \hat{n}_{k\sigma}, \quad \varepsilon_k = -2t \cos(\mathbf{q}_k \cdot \mathbf{a}_{jj'}), \quad (6.7)$$

where $\hat{n}_{k\sigma} \equiv \hat{c}_{k\sigma}^\dagger \hat{c}_{k\sigma}$ is the number operator for electrons of spin σ with momentum k , $\mathbf{a}_{jj'} \equiv \mathbf{r}_j - \mathbf{r}_{j'}$ is the lattice vector between any two neighboring sites in Λ , and ε_k heralds the triumphant return of the dispersion relation we derived in §3.2. The upshot is that \hat{H} decouples into independent momentum modes [24] and describes non-interacting band electrons with cosine-shaped “field” excitations forming the energy band.

Eigenstates and energies. Since \hat{H} decouples in k -space, let’s look at a single momentum mode. The Hamiltonian is $\hat{H}_k = (\varepsilon_k - \mu) \hat{n}_k$, and a suitable basis gives the spins present at each momentum: $\beta_k^* = \{|0\rangle_k, |\downarrow\rangle_k, |\uparrow\rangle_k, |2\rangle_k\}$. We see that \hat{H}_k acts diagonally:

$$\hat{H}_k |0\rangle = 0; \quad \hat{H}_k |\downarrow\rangle = (\varepsilon_k - \mu) |\downarrow\rangle; \quad \hat{H}_k |\uparrow\rangle = (\varepsilon_k - \mu) |\uparrow\rangle; \quad \hat{H}_k |2\rangle = 2(\varepsilon_k - \mu) |2\rangle. \quad (6.8)$$

Depending on k , ε_k may modulate from positive to negative; if k is known, then a detailed analysis of ground states similar to that of §5.1 may be carried out. Nevertheless, as long as $\varepsilon_k < \mu$, $|2\rangle$ will be the ground state; if $\varepsilon_k > \mu$, then the empty lattice is more energetically favorable. This is markedly different from the behavior of the $t = 0$ model, which relied on a balance between double occupancy and occupation, and did not depend on position. Here, the ground state is directly determined by the state’s momentum, but in a nontrivial way.

Full diagonalization. We choose a Bloch-like basis for the full Hilbert space which we call $\beta^* = \{|\sigma^*\rangle\}$, where $\sigma^* = (\sigma_1^*, \dots, \sigma_M^*)$ runs over the dual lattice Λ^* , and each entry $\sigma_k^* \in \{0, \downarrow, \uparrow, 2\}$ tells us how many electrons have a given momentum. Just as in §5.1, each \hat{n}_k acts independently on $|\sigma^*\rangle$, either killing or scaling the Fock state depending only on what is happening at quasimomentum k . The full Hamiltonian thus acts diagonally on β^* :

$$\hat{H} |\sigma^*\rangle = \left(\sum_k \varepsilon_k n_k - \mu N \right) |\sigma^*\rangle \equiv E |\sigma^*\rangle, \quad (6.9)$$

where $n_k = n_{k\uparrow} + n_{k\downarrow} \in \{0, 1, 2\}$ is the number of electrons at momentum k . Larger N lowers the energy, but if $\varepsilon_k > 0$, the momentum distribution within the lattice will raise the energy due to quantum fluctuations created by tunneling. If the Hubbard model is a quantum egg carton, then its Easter bunny must hop the right way for ε_k to minimize energy. In this sense, t is the danger of inadvertant heating if particles have the wrong speeds.

In one dimension with $a = 1$, $\varepsilon_k = -2t \cos(q)$ vanishes when $q = \pm\pi/2$, which reduces the model to the harmonic oscillator $\hat{H} = -\mu \hat{N}$. Meanwhile, ε_k takes extremal values $-2t$ when $q = 0$ and $+2t$ when $q = \pi$. (Other extrema are prevented because q is only defined on an interval—see §2.) Thus particles moving in one direction behave exactly as if they were moving in the opposite direction with the same speed. Since $\varepsilon_0 = -2t$, a ground state emerges at $q = 0$ [28]; this means that stationary particles hop most easily, but also that the tunneling energy benefit of this process is distinct from the motional energy due to q .

Statistical mechanics. Exact expressions for Z , E , and N are given in Appendix C, and are given for a single momentum mode. Since the single-mode model $\hat{H} = (\varepsilon_k - \mu)\hat{n}_k$ is proportional to the number operator, we can see that $E = \langle \hat{H} - \mu \hat{n}_k \rangle = \varepsilon_k N$.

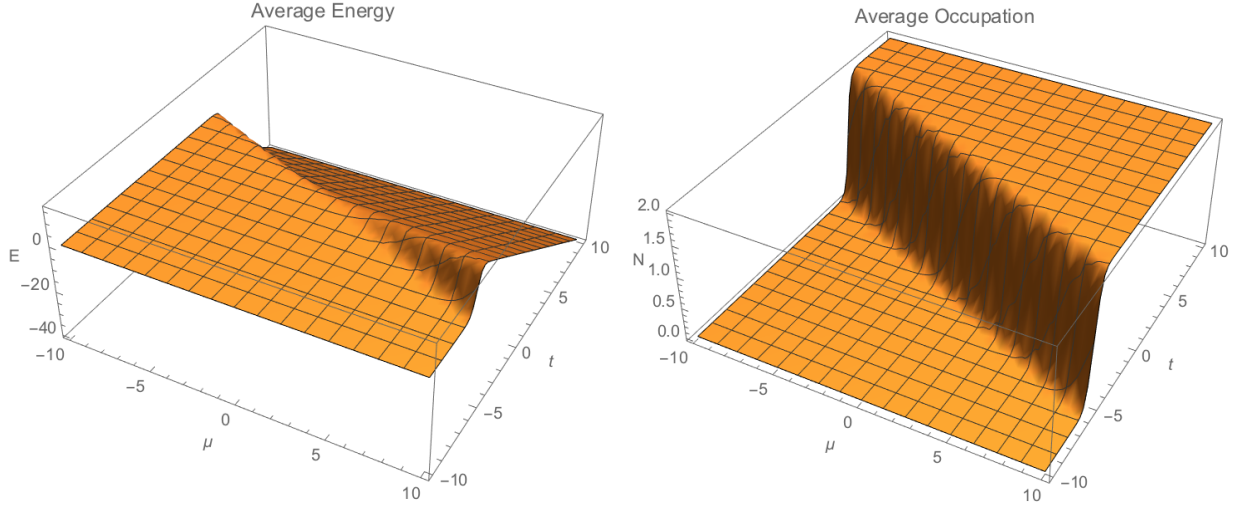


Figure 2: Average energy and density in the single-mode Fermi-Hubbard model at $\beta = 2$.

Graphs of E and N above show a ridge along $t = \mu/2$ corresponding to a sharp rise in occupation number; notably, there is no Mott gap. Evidently pure tunneling destroys the insulating behavior we saw earlier, but this is unsurprising. We'll return later to whether Mott behavior can survive in the presence of both t and U terms; for now let us move on.

7 The Bose-Hubbard Model

7.1 Single Site: Strong Interactions

The Hamiltonian. At $t = 0$, the Bose-Hubbard Hamiltonian is

$$\hat{H} = \frac{U}{2} \sum_j \hat{n}_j(\hat{n}_j - 1) - \mu \sum_j \hat{n}_j = \sum_j \hat{H}_j, \quad (7.1)$$

where $\hat{H}_j = \frac{U}{2}\hat{n}(\hat{n} - 1) - \mu\hat{n}$ is the one-site Hamiltonian. As in §5.1, we set out to solve this model first. In Pauli's absence, the single-site Hilbert space is infinite-dimensional, and is spanned by the Fock basis $\beta_j = \{|n\rangle_j\}$, where $n \in \mathbb{N}$ labels the number of bosons in the potential well. Luckily, \hat{H}_j acts on β_j diagonally:

$$\hat{H}_j |n\rangle = \left[\frac{U}{2}n(n-1) - \mu n \right] |n\rangle \equiv E(n) |n\rangle. \quad (7.2)$$

Eigenstates and energies. The energy scales quadratically with particle number, so if N is not fixed, then for $U < 0$ the spectrum is unbounded below, and there is no ground state with a finite number of particles. In practice, this is not an issue since optical lattices are loaded with a finite number of atoms, which would then condense in a single-well potential [26]. For a repulsive model, the energy minimum occurs when n is closest to

$$\frac{\partial E}{\partial n} \Big|_{\bar{n}} = U\bar{n} - \frac{U}{2} - \mu = 0 \implies \bar{n} = \frac{1}{2} + \frac{\mu}{U}. \quad (7.3)$$

In particular, $\bar{n} \in \mathbb{R}_{\geq 0}$ forces $\mu/U > -\frac{1}{2}$, and $U \geq 0$ (for the full Fock space) additionally bounds $\mu \geq -U/2$. Also, if $\mu/U \in \mathbb{Z}$, then \bar{n} is a half-integer equally far from two possible occupation numbers $n_0 = \frac{\mu}{U}$ (+1). By the symmetry of the energy parabola about its minimum, these occupations are degenerate ground states; moreover, every state is either unique or doubly degenerate. In the unique case, the ground state's energy is approximately

$$E_0 \approx E(\bar{n}) = \frac{U}{2} \left(\frac{1}{2} + \frac{\mu}{U} \right) \left[\left(\frac{1}{2} + \frac{\mu}{U} \right) - 1 \right] - \mu \left(\frac{1}{2} + \frac{\mu}{U} \right) = -\frac{(U+2\mu)^2}{8U}. \quad (7.4)$$

Meanwhile, in the degenerate case we have the exact result

$$E_0 = E(n_0) = \frac{U}{2} \frac{\mu}{U} \left[\frac{\mu}{U} - 1 \right] - \mu \frac{\mu}{U} = -\frac{\mu(U+\mu)}{2U}. \quad (7.5)$$

Comparing (7.4) and (7.5) shows that while the energy is always quadratic in μ , the extra $1/2$ changes its scaling from $\sim U + \frac{1}{U}$ (nondegenerate) to $\sim \frac{1}{U}$ (degenerate). The degree to which μ "is" a multiple of U thus controls the linear dependence of E_0 on interactions.

Mott phase. As we will see shortly, the ground state at fixed N is a Mott insulator [26]. It consists of $m \equiv \frac{N}{M} \in \mathbb{N}$ bosons occupying each lattice site, and following [27] it can be expressed as a product of Fock states, $|\psi_0\rangle = \prod_j (\hat{a}_j^\dagger)^m |0\rangle$.

Full diagonalization. For the full M -site Hilbert space, we choose the basis $\beta = \{|\mathbf{n}\rangle\}$, where $\mathbf{n} = (n_1, \dots, n_M)$ runs over $j \in \Lambda$, and each entry $n_j \in \mathbb{N}$ gives the occupation of site j . Each \hat{n}_j acts independently on $|\mathbf{n}\rangle$, so the Hamiltonian (7.1) is diagonal in this basis:

$$\hat{H} |\mathbf{n}\rangle = \left[\frac{U}{2} N(N-1) - \mu N \right] |\mathbf{n}\rangle \equiv E(N) |\mathbf{n}\rangle , \quad (7.6)$$

where N is the total number of bosons. In the absence of hopping, the ground state respects lattice site permutation symmetry, and is thus $(M!)$ -fold degenerate. Being site-independent, the ground state structure of \hat{H} is exactly as described above, with N replacing \hat{n}_j .

Statistical mechanics. The partition function, average energy, and average occupation number for a single site are infinite sums over $n \in \mathbb{N}$; their computation is rather involved, so see Appendix D. None of them have closed-form expressions, but the results are more elegant if we sum over \mathbb{Z} instead of \mathbb{N} , i.e. if we allow for negative bosonic occupations. (While unphysical, this is not a new idea [18].) In this case, Z takes the form of a Jacobi theta function [20], and as $\beta \rightarrow 0$ we can take advantage of the fact that $E(n)$ is quadratic in n to regard $e^{-\beta E(n)}$ as a Gaussian. This turns N and E into Gaussian integrals that can be evaluated explicitly. Alternatively, we may settle for nonnegative occupations, cut off the sums after (e.g.) $n = 100$, and evaluate numerically. Below are plots of N and E evaluated using this cutoff, which becomes an excellent approximation at lower temperature.

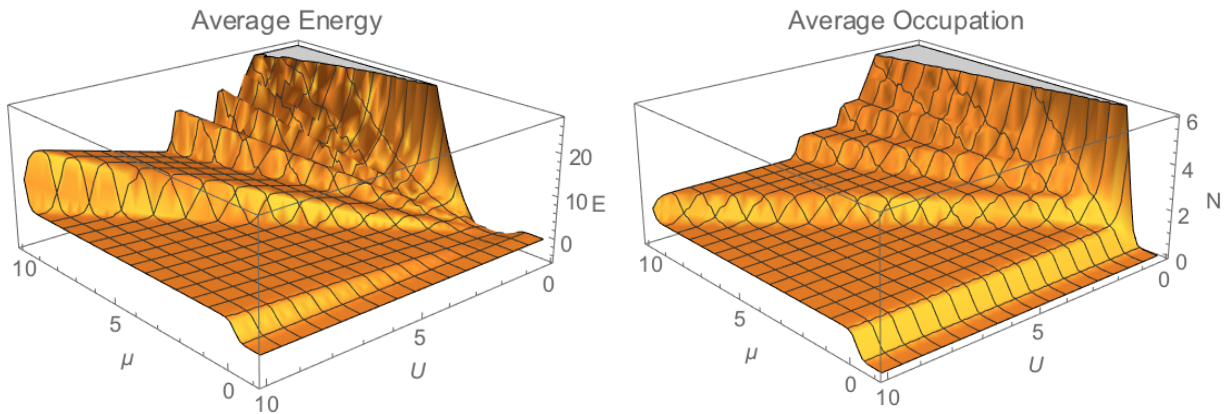


Figure 3: Average energy and density in the single-site Bose-Hubbard model at $\beta = 10$.

The most important feature of both graphs above is their similarity to those presented in §5.1: both the Fermi and Bose Hamiltonians exhibit the same energy ridges and Mott gaps at $t = 0$. The Bose-Hubbard model accommodates arbitrarily many bosons, so it exhibits infinitely many Mott plateaus. Notably, the graphs above only show the region $\mu, U \geq 0$: as mentioned above, attractive interactions $U < 0$ pose problems for the energy spectrum of the model if N is not fixed—the system tries to put an infinite number of bosons in the site. The energy landscape and average occupation become more jagged at large μ/U , suggesting that weakly repulsive models are more sensitive to perturbations in the lattice's filling, such as impurities or imperfections. Finally, note that in Bose-Hubbard physics there is no such thing as half-filling, since the occupation per site N/M is unbounded.

7.2 Tight Binding: Weak Interactions

We shall see that the $U = 0$ Bose-Hubbard model behaves almost identically to the $U = 0$ Fermi-Hubbard model; therefore we will move quickly through this section.

Analysis. At $U = 0$, the Bose-Hubbard Hamiltonian is

$$\hat{H} = -t \sum_{\langle ij \rangle} (\hat{a}_i^\dagger \hat{a}_j + \hat{a}_j^\dagger \hat{a}_i) - \mu \sum_j \hat{n}_j. \quad (7.7)$$

We define k -space operators exactly as in (6.5–6.6) but without spin labels, substitute them into \hat{H} , and obtain—by the same algebra as in Appendix C—the decoupled form

$$\hat{H} = \sum_k (\varepsilon_k - \mu) \hat{n}_k, \quad \varepsilon_k = -2t \cos(ka). \quad (7.8)$$

In a single mode of momentum k , a basis is given by $\beta_k^* = \{|n^*\rangle\}$, where n^* is the number of bosons occupying that mode. The Hamiltonian $\hat{H}_k = (\varepsilon_k - \mu) \hat{n}_k$ acts diagonally on β_k^* :

$$\hat{H}_k |n^*\rangle = (\varepsilon_k - \mu) n^* |n^*\rangle \equiv E(n^*) |n^*\rangle. \quad (7.9)$$

As before, the relative sizes of ε_k and μ determine the ground state; but since n is unbounded, $\varepsilon_k < \mu$ will cause a Bose catastrophe like the one described above in the case $t = 0$, $U < 0$. No such catastrophe occurs, however, if bosons fill the lattice at just the right momenta for the tunneling coefficient to stay ahead of μ . In any case, a basis for the full $U = 0$ model is given by $\beta^* = \{|\mathbf{n}^*\rangle\}$, where $\mathbf{n}^* = (n_1^*, \dots, n_M^*)$ runs over Λ^* , and each n_k^* gives the occupation number of mode k . The full Hamiltonian acts diagonally on β^* :

$$\hat{H} |\mathbf{n}^*\rangle = \left(\sum_k \varepsilon_k n_k - \mu N \right) |\mathbf{n}^*\rangle \equiv E |\mathbf{n}^*\rangle. \quad (7.10)$$

The ground state and energy structure of this model is more or less the same as that of §5.2.

It should be noted that the single-mode Hamiltonian is identical to a harmonic oscillator with energy $\varepsilon_k - \mu$. Its energies and statistical mechanics are also equivalent, but for completeness the results for Z , E , and N are in Appendix D. The ridges and jumps in Fig. 2 become divergent when infinitely many bosons are allowed to contribute to the system's energy; otherwise, the structure the $t - \mu$ landscape is the same as in the Fermi case.

Phase transition. Whereas the $t = 0$ ground state was a Mott insulator, the $U = 0$ ground state is a superfluid [27]. All N bosons crowd into the $q = 0$ Bloch wave, so

$$|\psi_0\rangle = \frac{(\hat{a}_{q=0}^\dagger)^N}{\sqrt{N!}} |0\rangle \rightarrow e^{\sqrt{N} \hat{a}_{q=0}^\dagger} |0\rangle = \exp \left(\sqrt{\frac{N}{M}} \sum_{j \in \Lambda} \hat{a}_j^\dagger \right) |0\rangle = \prod_{j \in \Lambda} \exp \left(\sqrt{\frac{N}{M}} \hat{a}_j^\dagger \right) |0\rangle. \quad (7.11)$$

This describes a coherent state, with Poissonian occupation number fluctuations, notably larger than the “number-squeezed” $t = 0$ ground state [27].

At some critical ratio $(U/t)_c$, a second-order phase transition from superfluid to Mott insulator occurs [11]; we will not pursue this any further, but it is crucial to highlight that even the bare-bones Hubbard Hamiltonian exhibits such rich and complex behavior.

Part III

Lattice Limits

Table of Contents

8 Two Sites: Fermi-Hubbard	26
8.1 One Electron	26
8.2 Two Electrons	27
8.3 Three Electrons	28
8.4 Complete Solution	29
9 Two Sites: Bose-Hubbard	33
9.1 One and Two Bosons	33
9.2 Many Bosons	35
9.3 High-Temperature Limit	36
10 Conclusions and Outlook	38

We now drastically change our perspective. Having just finished analyzing the limiting (non)interacting behavior of the Hubbard model, we will now attempt to capture the full behavior of both the t and U terms of the Hamiltonian: we will do so by restricting to very small lattices, which yield to analytic methods. The case of zero lattice sites is trivial since $\hat{H} = 0$, while the case of one site is equivalent to the analysis we carried out in the atomic limit $t = 0$, i.e. in §6.1 and §7.1 above.

We therefore concern ourselves in the next two sections with two-site models for both fermions and bosons. Our strategy will be to take advantage of particle number conservation, which splits the full 2-site Hilbert space into a direct sum of subspaces of fixed N . To completely solve the system, it suffices to diagonalize the Hamiltonian at fixed N , for each N . In the Fermi case, a maximum of 4 particles (2 paired spins in each site) populate the lattice, while the bosonic model allows arbitrary occupations.

8 Two Sites: Fermi-Hubbard

We begin with the full 2-site Fermi-Hubbard Hamiltonian, written out in full gore and glory:

$$\begin{aligned}\hat{H}_F^{(2)} = & -t(\hat{c}_{1\uparrow}^\dagger \hat{c}_{2\uparrow} + \hat{c}_{1\downarrow}^\dagger \hat{c}_{2\downarrow} + \hat{c}_{2\uparrow}^\dagger \hat{c}_{1\uparrow} + \hat{c}_{2\downarrow}^\dagger \hat{c}_{1\downarrow}) + \\ & + U(\hat{n}_{1\uparrow} \hat{n}_{1\downarrow} + \hat{n}_{2\uparrow} \hat{n}_{2\downarrow}) - \mu(\hat{n}_{1\uparrow} + \hat{n}_{1\downarrow} + \hat{n}_{2\uparrow} + \hat{n}_{2\downarrow}).\end{aligned}\quad (8.1)$$

Each lattice site may be either empty, occupied by an electron of spin up or down, or doubly occupied. With 4 possibilities on each of 2 lattice sites, the Hilbert space of the system has dimension $2^4 = 16$ [13]. Luckily, we can avoid 16×16 matrices by working in sectors of fixed particle number $N \in \{0, 1, 2, 3, 4\}$. We first embark on a detailed analysis of the physically interesting cases $N = 1, 2, 3$, and then assemble the complete solution.

8.1 One Electron

A convenient basis for the single-particle sector is given by labeling the possible spins and locations of the sites: $\beta = \{|\downarrow_1\rangle, |\uparrow_1\rangle, |\downarrow_2\rangle, |\uparrow_2\rangle\}$. There is no double occupancy, so we ignore the U term in (8.1); moreover, $N = 1$ gives energy $-\mu$ to each state. Then \hat{H} acts on β by

$$\left. \begin{aligned}\hat{H} |\downarrow_1\rangle &= -t |\downarrow_2\rangle - \mu |\downarrow_1\rangle \\ \hat{H} |\uparrow_1\rangle &= -t |\uparrow_2\rangle - \mu |\uparrow_1\rangle \\ \hat{H} |\downarrow_2\rangle &= -t |\downarrow_1\rangle - \mu |\downarrow_2\rangle \\ \hat{H} |\uparrow_2\rangle &= -t |\uparrow_1\rangle - \mu |\uparrow_2\rangle\end{aligned}\right\} \implies \hat{H}_1 = -\begin{pmatrix} -\mu & 0 & -t & 0 \\ 0 & -\mu & 0 & -t \\ -t & 0 & -\mu & 0 \\ 0 & -t & 0 & -\mu \end{pmatrix} = -t \hat{K}_1 - \mu \mathbb{1}_4,$$

where $\hat{K}_1 = \begin{pmatrix} 0 & 0 & 1 & 0 \\ 0 & 0 & 0 & 1 \\ 1 & 0 & 0 & 0 \\ 0 & 1 & 0 & 0 \end{pmatrix}.$

(8.2)

The diagonalization of \hat{H}_1 is accomplished by the eigenbasis $\beta_* = \{|\sigma_\pm\rangle\}$, defined by

$$|\downarrow_\pm\rangle = \frac{1}{\sqrt{2}}(|\downarrow_2\rangle \pm |\downarrow_1\rangle); \quad |\uparrow_\pm\rangle = \frac{1}{\sqrt{2}}(|\uparrow_2\rangle \pm |\uparrow_1\rangle).$$
(8.3)

These states resolve spin but not site, which makes sense for a model with no interactions. Their respective energies, however, do not depend on spin:

$$\left. \begin{aligned}\hat{H}_1 |\downarrow_\pm\rangle &= (\mp t - \mu) |\downarrow_\pm\rangle \\ \hat{H}_1 |\uparrow_\pm\rangle &= (\mp t - \mu) |\uparrow_\pm\rangle\end{aligned}\right\} \implies E(\sigma_\pm) = \mp t - \mu.$$
(8.4)

If $t > 0$, then $|\sigma_+\rangle$ are doubly degenerate ground states, while if $t < 0$, then $|\sigma_-\rangle$ are.

The partition function and average energy are simple, but as a matter of principle we relegate them to Appendix E. Assuming $t > 0$, the (grand-canonical) average energy is unsurprisingly lowered roughly linearly with increasing t ; it is also independent of μ .

8.2 Two Electrons

The Hamiltonian. The 2-particle sector of the 2-site model is the most interesting: it describes half-filling and has a 6-dimensional Hilbert space spanned by the site-spin basis

$$\beta = \{|02\rangle, |\downarrow\downarrow\rangle, |\downarrow\uparrow\rangle, |\uparrow\downarrow\rangle, |\uparrow\uparrow\rangle, |20\rangle\}. \quad (8.5)$$

The Hamiltonian acts on this basis in an interesting manner:

$$\left. \begin{aligned} \hat{H} |02\rangle &= -t(|\uparrow\downarrow\rangle + |\downarrow\uparrow\rangle) \\ &\quad + (U - 2\mu) |02\rangle \\ \hat{H} |\downarrow\downarrow\rangle &= -2\mu |\downarrow\downarrow\rangle \\ \hat{H} |\downarrow\uparrow\rangle &= -t(|20\rangle + |02\rangle) - 2\mu |\downarrow\uparrow\rangle \\ \hat{H} |\uparrow\downarrow\rangle &= -t(|02\rangle + |20\rangle) - 2\mu |\uparrow\downarrow\rangle \\ \hat{H} |\uparrow\uparrow\rangle &= -2\mu |\uparrow\uparrow\rangle \\ \hat{H} |20\rangle &= -t(|\downarrow\uparrow\rangle + |\uparrow\downarrow\rangle) \\ &\quad + (U - 2\mu) |20\rangle \end{aligned} \right\} \Rightarrow \left\{ \begin{array}{l} \hat{H}_2 = -t\hat{K}_2 - 2\mu\mathbb{1}_6, \\ \hat{K}_2 = \begin{pmatrix} -\frac{U}{t} & 0 & 1 & 1 & 0 & 0 \\ 0 & 0 & 0 & 0 & 0 & 0 \\ 1 & 0 & 0 & 0 & 0 & 1 \\ 1 & 0 & 0 & 0 & 0 & 1 \\ 0 & 0 & 0 & 0 & 0 & 0 \\ 0 & 0 & 1 & 1 & 0 & -\frac{U}{t} \end{pmatrix}. \end{array} \right. \quad (8.6)$$

Diagonalization and eigenstates. Diagonalizing \hat{H}_2 , we find an eigenbasis of states:

$$\beta_* = \{|\downarrow\downarrow\rangle, |\uparrow\uparrow\rangle, |1-\rangle, |2-\rangle, |\psi_+\rangle, |\psi_-\rangle\}. \quad (8.7)$$

Here $|\downarrow\downarrow\rangle$ and $|\uparrow\uparrow\rangle$ are unchanged from above, and $|1-\rangle$ and $|2-\rangle$ are even mixtures of the unpaired and paired states, respectively. Three of these four eigenstates are degenerate, since their energies contain no tunneling energy contributions:

$$\begin{aligned} \hat{H}_2 |\downarrow\downarrow\rangle &= -2\mu |\downarrow\downarrow\rangle; & \hat{H}_2 |\uparrow\uparrow\rangle &= -2\mu |\uparrow\uparrow\rangle; \\ \hat{H}_2 |1-\rangle &\equiv \hat{H}\left[\frac{1}{\sqrt{2}}(|\uparrow\downarrow\rangle - |\downarrow\uparrow\rangle)\right] = -2\mu |1-\rangle; \\ \hat{H}_2 |2-\rangle &\equiv \hat{H}\left[\frac{1}{\sqrt{2}}(|20\rangle - |02\rangle)\right] = (U - 2\mu) |2-\rangle. \end{aligned} \quad (8.8)$$

The last two eigenstates are more complicated mixtures of states. To describe them, we introduce the dimensionless coupling constant $\gamma \equiv U/4t$ and the function

$$\phi_{\pm}(t, U) = \frac{U \pm \sqrt{16t^2 + U^2}}{4t} = \gamma \pm \sqrt{1 + \gamma^2} \equiv \phi_{\pm}(\gamma). \quad (8.9)$$

The states $|\psi_{\pm}\rangle$ contain an admixture of the superpositions $|20\rangle + |02\rangle$ and $|\uparrow\downarrow\rangle + |\downarrow\uparrow\rangle$ whose relative proportions are fixed by $\phi_{\pm}(\gamma)$ [28]. More precisely,

$$|\psi_{\pm}\rangle = \mathcal{N}_{\pm} \left[(|20\rangle + |02\rangle) \pm \phi_{\pm}^{\pm 1}(\gamma) (|\uparrow\downarrow\rangle + |\downarrow\uparrow\rangle) \right], \quad (8.10)$$

where \mathcal{N}_\pm is a normalization constant determined by $\langle \psi_\pm | \psi_\pm \rangle = 1$. Explicitly, we have

$$\begin{aligned}\mathcal{N}_+^2 [2 + 2\phi_+^2(\gamma)] &= 1 \implies \mathcal{N}_+ = \frac{1}{2} \frac{1}{\sqrt{1 + \gamma\phi_+(\gamma)}}; \\ \mathcal{N}_-^2 [2 + 2\phi_+^{-2}(\gamma)] &= 1 \implies \mathcal{N}_- = \frac{1}{2} \sqrt{\frac{1 + \frac{1}{2}\gamma\phi_+(\gamma)}{1 + \gamma\phi_+(\gamma)}}.\end{aligned}\quad (8.11)$$

The energies of these last two states are expressed in terms of ϕ_\pm :

$$\hat{H}_2 |\psi_\pm\rangle = \left[\frac{1}{2} (U \mp \sqrt{16t^2 + U^2}) - 2\mu \right] |\psi_\pm\rangle = 2(t\phi_\mp(\gamma) - \mu) |\psi_\pm\rangle \equiv E_\pm |\psi_\pm\rangle. \quad (8.12)$$

All things energy. The energy differences between the 6 eigenstates are determined by γ . Relative to -2μ , three states have energy 0; one has energy $U = 4t\gamma$; and two have energy $2t\phi_\mp(\gamma)$. Noting that $\sqrt{1 + \gamma^2} > |\gamma| \geq \gamma$, one can check that $|\psi_+\rangle$ is the ground state for $t > 0$, while $|\psi_-\rangle$ has the lowest energy when $t < 0$. As before, exact expressions for Z and E are collected in Appendix E; we will return to them in a more complete analysis of the 2-site model's statistical mechanics.

8.3 Three Electrons

The three-particle subspace is composed of states with two spins paired on a site and one spin unpaired. The basis for this space can thus be labeled by the position and spin of the lone electron, making it isomorphic to the $N = 1$ subspace:

$$\beta = \{|\downarrow 2\rangle, |\uparrow 2\rangle, |2\downarrow\rangle, |2\uparrow\rangle\} = \{|\downarrow_1\rangle, |\uparrow_1\rangle, |\downarrow_2\rangle, |\uparrow_2\rangle\}. \quad (8.13)$$

(More physically, this isomorphism follows from particle-hole symmetry [8].) The Hamiltonian acts on β by leaving $U - 3\mu$ along the diagonal and by hopping states as in §8.1:

$$\left. \begin{aligned}\hat{H} |\downarrow_1\rangle &= -t |\downarrow_2\rangle + (U - 3\mu) |\downarrow_1\rangle \\ \hat{H} |\uparrow_1\rangle &= -t |\uparrow_2\rangle + (U - 3\mu) |\uparrow_1\rangle \\ \hat{H} |\downarrow_2\rangle &= -t |\downarrow_1\rangle + (U - 3\mu) |\downarrow_2\rangle \\ \hat{H} |\uparrow_2\rangle &= -t |\uparrow_1\rangle + (U - 3\mu) |\uparrow_2\rangle\end{aligned} \right\} \implies \hat{H}_1 = \begin{pmatrix} U - 3\mu & 0 & -t & 0 \\ 0 & U - 3\mu & 0 & -t \\ -t & 0 & U - 3\mu & 0 \\ 0 & -t & 0 & U - 3\mu \end{pmatrix} = -t \hat{K}_1 + (U - 3\mu) \mathbb{1}_4, \quad (8.14)$$

where \hat{K}_1 is the matrix defined in (8.2). We diagonalize this model using the doubly degenerate eigenbasis $\beta_* = \{|\sigma_\pm\rangle\}$ defined in (8.3), which yields spin-independent energies

$$\hat{H}_3 |\sigma_\pm\rangle = \left[\mp t + (U - 3\mu) \right] |\sigma_\pm\rangle \equiv E_\pm |\sigma_\pm\rangle. \quad (8.15)$$

Hence the 3-particle sector behaves almost exactly like the 1-site sector, including its statistical mechanics (see Appendix E), except for the addition of U in all of the energies.

8.4 Complete Solution

We are now ready to assemble the complete solution to the 2-site Fermi-Hubbard model. As mentioned above, its full Hilbert space \mathcal{H} is 16-dimensional. Because $[\hat{H}, \hat{N}] = 0$, the full space \mathcal{H} decomposes as a direct sum of subspaces of fixed particle number:

$$\mathcal{H} = \mathcal{H}_0 \oplus \mathcal{H}_1 \oplus \mathcal{H}_2 \oplus \mathcal{H}_3 \oplus \mathcal{H}_4. \quad (8.16)$$

State structure. The one-dimensional subspaces \mathcal{H}_0 and \mathcal{H}_4 describe an empty and a completely filled lattice, respectively. They have no dynamics, and are barren one-dimensional outposts of \mathcal{H} where nothing happens. As discussed above, the 4-dimensional sectors \mathcal{H}_1 and \mathcal{H}_3 behave identically, while the 6-dimensional half-filled sector \mathcal{H}_2 is most nontrivial.

Statistical mechanics. Let $\mathcal{H} = \mathcal{H}^a \oplus \mathcal{H}^b$ be a Hilbert space that decomposes as a direct sum of two pieces, and let \hat{H} be a Hamiltonian acting on \mathcal{H} . Given energy eigenbases $\mathcal{B}^a = \{|\psi_k^a\rangle\}$ and $\mathcal{B}^b = \{|\psi_{k'}^b\rangle\}$ for \mathcal{H}^a and \mathcal{H}^b respectively, their union is an \hat{H} -eigenbasis for all of \mathcal{H} . Then the partition function for \hat{H} over all of \mathcal{H} is the *sum* of the individual partition functions for \mathcal{H}^a and \mathcal{H}^b :

$$Z = \sum_{\alpha \in \mathcal{B}^a \cup \mathcal{B}^b} e^{\beta E_\alpha} = \sum_{k \in \mathcal{B}^a} e^{-\beta E_k} + \sum_{k' \in \mathcal{B}^b} e^{-\beta E_{k'}} = Z^a + Z^b. \quad (8.17)$$

This is markedly different from the usual decomposition of Z as a product, which occurs when \mathcal{H} is composed of several noninteracting subsystems [25]. Instead, we are simply computing Z by summing over independent subspaces of \mathcal{H} .

In the case at hand, the partition function for the 2-site model is the sum of the fixed- N partition functions, $Z = Z_0 + Z_1 + Z_2 + Z_3 + Z_4$. (See Appendix E for the exact analytical expression.) The average energy is unfortunately not so simple to compute: one may either manually add up $(E_\alpha + \mu N)e^{-\beta E_\alpha}$ (where α runs over all 16 eigenstates of the 2-site model) and divide by Z , or alternatively one may compute $E = \frac{\partial}{\partial \beta}(\log Z)$ from the partition function. We are more lucky with N : since particle number is fixed on each subspace,

$$N = \frac{1}{Z} \sum_{\alpha} N_{\alpha} e^{-\beta E_{\alpha}} = \frac{1}{Z} \sum_{n=0}^4 n Z_n = \frac{Z_1 + 2Z_2 + 3Z_3 + 4Z_4}{Z_0 + Z_1 + Z_2 + Z_3 + Z_4}. \quad (8.18)$$

The point here is that the partition functions Z_n give us everything we need to know about the system, and the results are written down in Appendix E and plotted below. The first page of figures shows N and E as functions of U plotted against μ for various values of t ; the second page shows $N(t, \mu)$ and $E(t, \mu)$ for various values of U . For clarity, the plots are restricted to the quadrant $U, t, \mu > 0$.

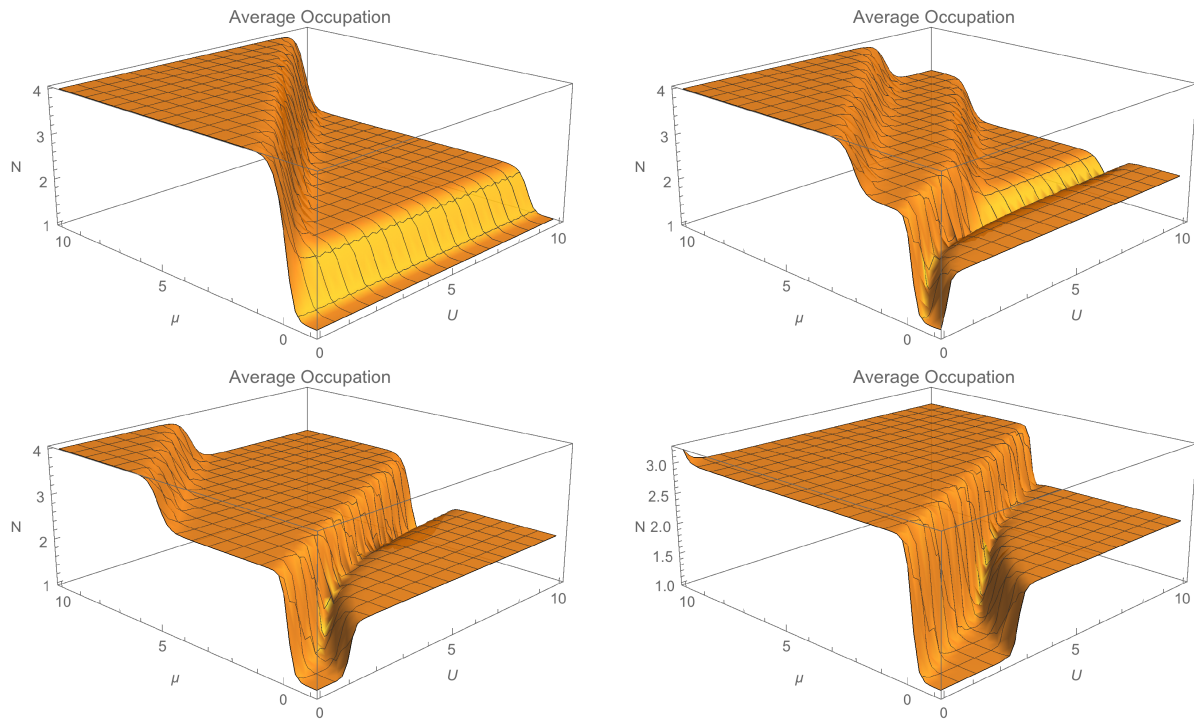


Figure 4: Occupation $N(U, \mu)$ at temperature $\beta = 5$ for tunneling coefficients $t = 0, 2, 5, 10$.

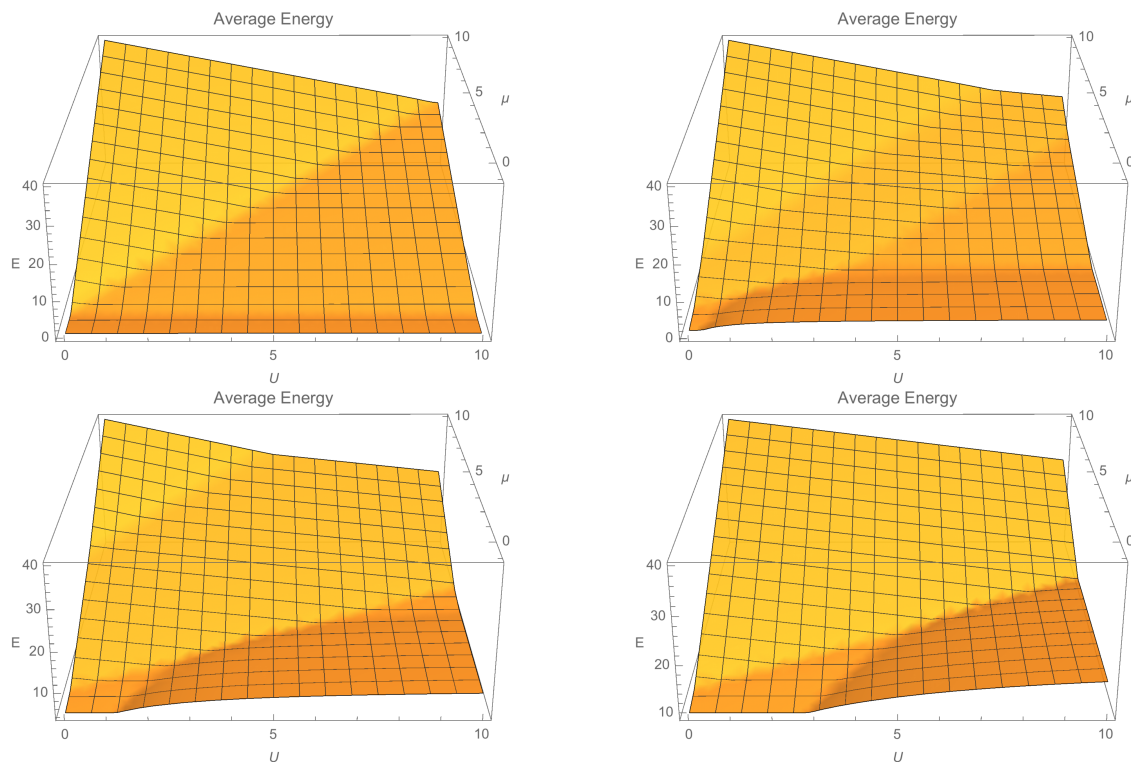


Figure 5: Energy $E(U, \mu)$ at temperature $\beta = 5$ for tunneling coefficients $t = 0, 2, 5, 10$.

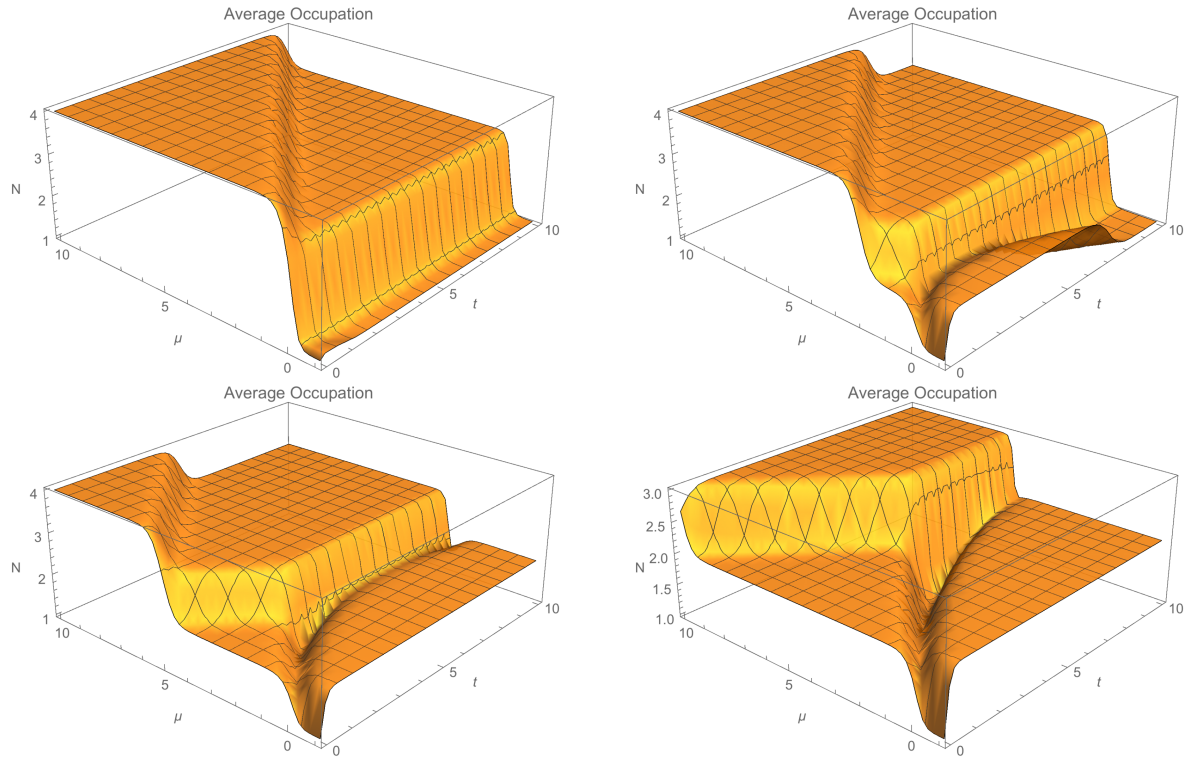


Figure 6: Occupation $N(t, \mu)$ at temperature $\beta = 5$ for interaction energies $U = 0, 2, 5, 10$.

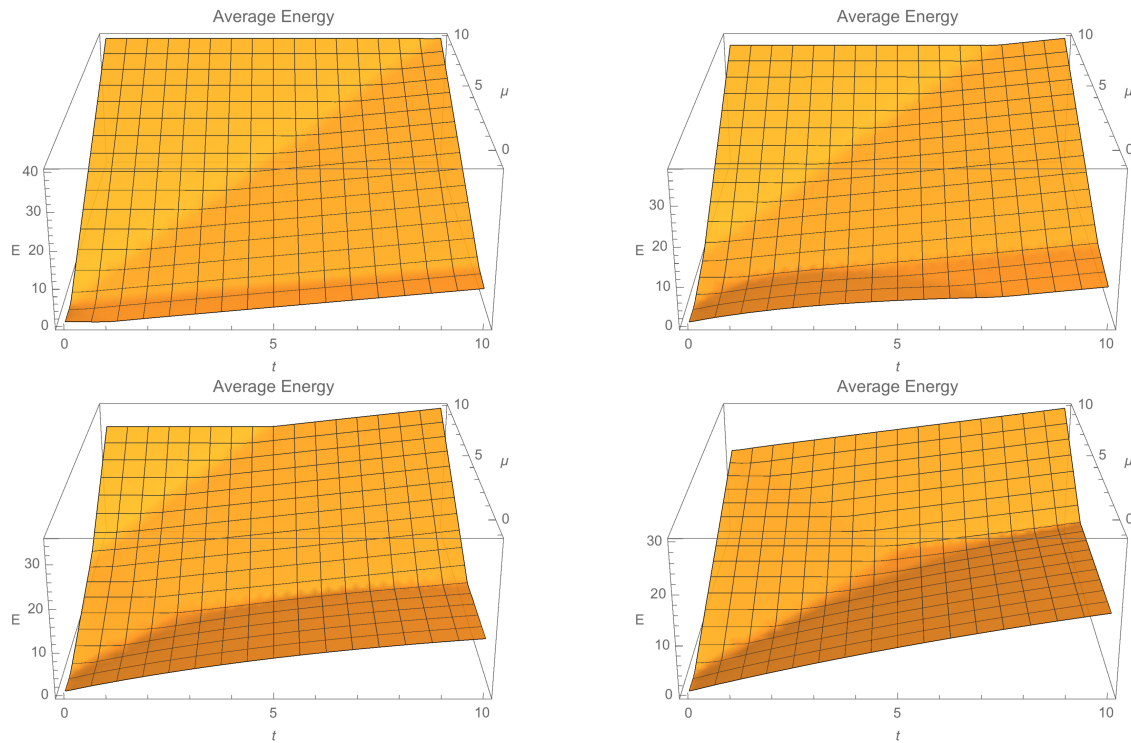


Figure 7: Energy $E(t, \mu)$ at temperature $\beta = 5$ for interaction energies $U = 0, 2, 5, 10$.

Discussion. The most immediate observation is that the plots of mean energy look more or less like faint echoes of their corresponding occupation number plots: their ridge lines lie in the same places, and their gradients correspond to the average particle number for each value of (U, t, μ) , i.e. $|\nabla E| \sim N$. This tells us that (1) we can focus on N as an indicator of the system's state structure; and (2) the filling of the lattice is the main driver of changes in its energy content and hence of its thermodynamic properties [24].

In Fig. 4, a clearly visible Mott plateau at $t = 0$ exactly matches the one shown in Fig. 1. As t rises, this plateau splits into two sublevels $N = 3, 4$ and a ditch of $N = 1$ forms along the line $\mu = 0$ between two regions of half-filling. This ditch becomes a valley, and the $N = 3$ plateau merges with the valley while the $N = 4$ plateau drifts off to $\mu \rightarrow \infty$. While strong tunneling eventually washes out Mott-like behavior, t -dominated models do exhibit a *hopping*-induced insulating region near $(U, \mu) = (0, 0)$. Here the lattice typically accommodates a single fermion, until the addition of an energy $\mu = U/2$ causes the occupancy to jump to 3. The stronger the tunneling, the larger this region, and the more energy must be added before the lattice fills up completely.

Figure 5 shows the model's t -dependence explicitly. At weak coupling $U \rightarrow 0$, the jump from $N = 1$ to $N = 3$ described above is clearly visible. Ramping up the repulsion reveals the expected emergence of a region of half-filling, which is preferred by strong- U models, near $(t, \mu) = (0, 0)$. Less expectedly, however, a second such region also forms at larger values of μ ; this plateau may be attributed to Mott-like causes because of its appearance as $t \rightarrow 0$ [28]. Separating the two regions is a ditch, one of whose key features is its refusal to dip below $N = 1$: unlike the 1-site ($t = 0$) model, nowhere in the parameter space of the 2-site model is an empty lattice the ground state. Perhaps the number of lattice sites acts as a “geometric chemical potential” raising the system’s occupancy.

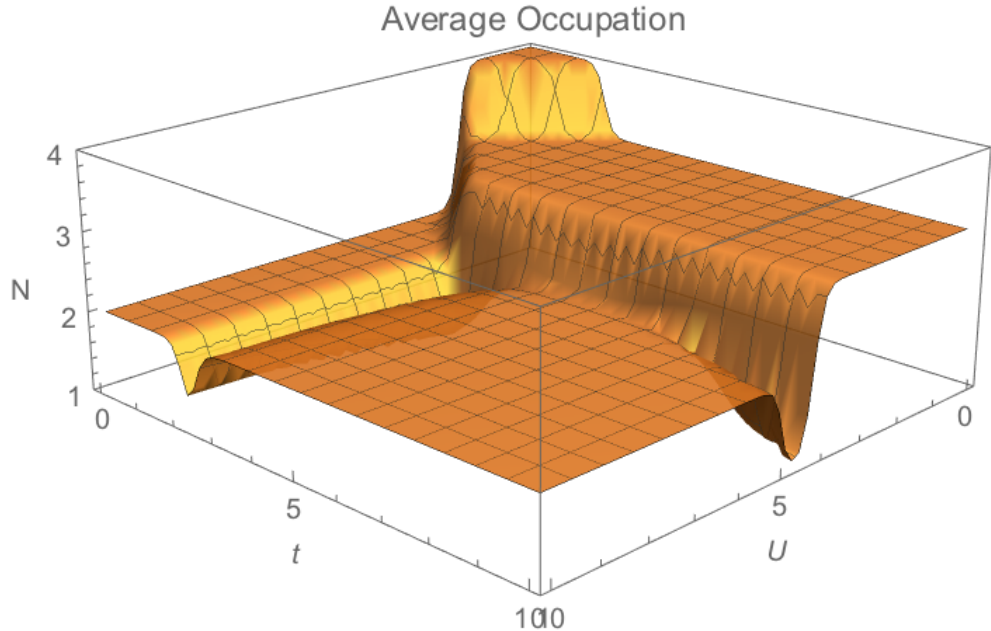


Figure 8: Bonus: occupation $N(U, t)$ at $\beta = 10$ with chemical potential $\mu = 2$.

9 Two Sites: Bose-Hubbard

Much like several remote cultures, atomic physicists count “one—two—many.” Taking inspiration from this witticism [10], we will solve the 2-site Bose-Hubbard model first for one and two bosons, then generalize to arbitrary (but fixed) N . As in the Fermi case, the “complete solution” to the 2-site model is the direct sum of the results from each fixed- N case. Since arbitrarily many bosons are allowed into the lattice, the corresponding Fock space is infinite-dimensional; this will not faze us, however, as we set out to determine its properties.

The 2-site Bose-Hubbard Hamiltonian is

$$\hat{H}_{\text{B}}^{(2)} = -t(\hat{a}_1^\dagger \hat{a}_2 + \hat{a}_2^\dagger \hat{a}_1) + \frac{U}{2}(\hat{n}_1(\hat{n}_1 - 1) + \hat{n}_2(\hat{n}_2 - 1)) - \mu(\hat{n}_1 + \hat{n}_2). \quad (9.1)$$

Each lattice site can hold an arbitrary number of bosons, so we may label states by their occupation: thus a basis for the many-body Fock space is given by $\beta = \{|n_1, n_2\rangle\}$, with $n_1, n_2 \in \mathbb{N}$ [7]. At first, however, let us be more modest.

9.1 One and Two Bosons

One boson. A single boson can occupy either of the two lattice sites, so $\beta = \{|01\rangle, |10\rangle\}$ forms a basis for the state space. The Hamiltonian acts by

$$\left. \begin{aligned} \hat{H}|01\rangle &= -t|10\rangle - \mu|01\rangle \\ \hat{H}|10\rangle &= -t|01\rangle - \mu|10\rangle \end{aligned} \right\} \implies \hat{H}_1 = -\begin{pmatrix} \mu & t \\ t & \mu \end{pmatrix} = -t\hat{\sigma}_1 - \mu\mathbb{1}_2, \quad (9.2)$$

where $\hat{\sigma}_1$ is the first Pauli matrix. The eigenstates of \hat{H}_1 and their energies are

$$|\psi_{\pm}\rangle \equiv \frac{1}{\sqrt{2}}(|10\rangle \pm |01\rangle), \quad \hat{H}|\psi_{\pm}\rangle = (\mp t - \mu)|\psi_{\pm}\rangle. \quad (9.3)$$

If $t > 0$, then ψ_+ is the ground state; if $t < 0$, ψ_- is. At $t = 0$, the states are degenerate.

Two bosons. With two bosons on the lattice, the system allows the independent states $\beta = \{|02\rangle, |11\rangle, |20\rangle\}$. The Hamiltonian acts on these by

$$\left. \begin{aligned} \hat{H}|02\rangle &= -t|11\rangle + (U - 2\mu)|02\rangle \\ \hat{H}|11\rangle &= -t(|02\rangle + |20\rangle) - 2\mu|11\rangle \\ \hat{H}|20\rangle &= -t|11\rangle + (U - 2\mu)|20\rangle \end{aligned} \right\} \implies \begin{cases} \hat{H}_2 = -t\hat{K} - 2\mu\mathbb{1}_3, \\ \hat{K} = \begin{pmatrix} -\frac{U}{t} & 1 & 0 \\ 1 & 0 & 1 \\ 0 & 1 & -\frac{U}{t} \end{pmatrix}. \end{cases} \quad (9.4)$$

We diagonalize \hat{H}_2 to find an eigenbasis $\beta_* = \{|\psi_0\rangle, |\psi_+\rangle, |\psi_-\rangle\}$. The first eigenstate is an equal mixture of doubly occupied states:

$$|\psi_0\rangle \equiv \frac{1}{\sqrt{2}}(|20\rangle - |02\rangle), \quad \hat{H}_2|\psi_0\rangle = (U - 2\mu)|\psi_0\rangle \equiv E_0|\psi_0\rangle. \quad (9.5)$$

To define $|\psi_{\pm}\rangle$, we need a new coupling constant $g \equiv U/2t$ and a function similar to ϕ_{\pm} :

$$f_{\pm}(t, U) = \frac{U \pm \sqrt{8t^2 + U^2}}{2t} = g \pm \sqrt{2 + g^2} \equiv f_{\pm}(g). \quad (9.6)$$

Then states $|\psi_{\pm}\rangle$ are defined [28] by

$$|\psi_{\pm}\rangle = \mathcal{N}_{\pm} \left[(|02\rangle + |20\rangle) + f_{\pm}(g) |11\rangle \right], \quad (9.7)$$

where \mathcal{N}_{\pm} is a normalization constant given by

$$\langle \psi_{\pm} | \psi_{\pm} \rangle = 1 \implies \mathcal{N}^2 [2 + f_{\pm}^2(g)] = 1 \implies \mathcal{N}_{\pm} = \frac{1}{\sqrt{2g(2 + f_{\pm}(g))}}. \quad (9.8)$$

And as in the Fermi case, the energies of $|\psi_{\pm}\rangle$ are determined by f_{\pm} :

$$\hat{H}_2 |\psi_{\pm}\rangle = \left[\frac{1}{2} (U \mp \sqrt{8t^2 + U^2}) - 2\mu \right] |\psi_{\pm}\rangle = (tf_{\mp}(g) - 2\mu) |\psi_{\pm}\rangle \equiv E_{\pm} |\psi_{\pm}\rangle. \quad (9.9)$$

However, the ground state structure is different than in the Fermi model, as shown below.

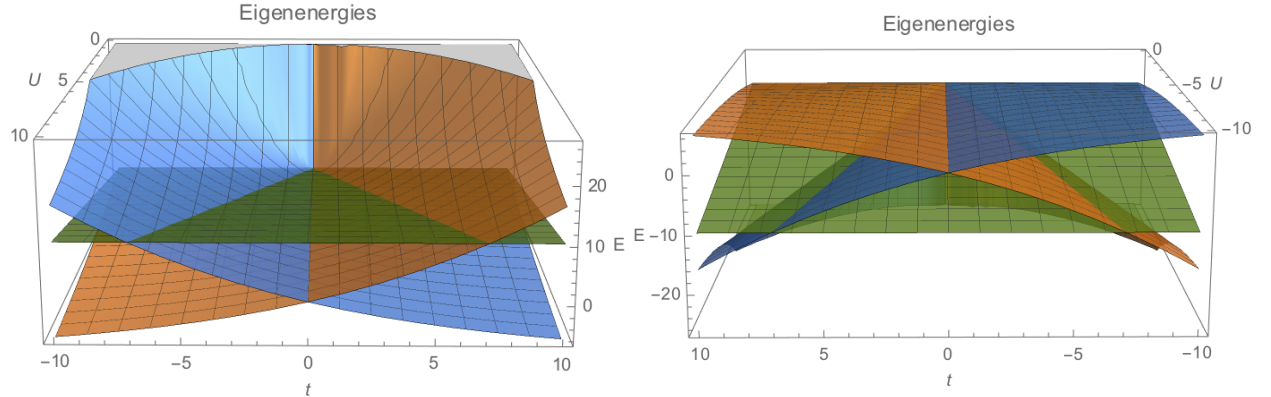


Figure 9: Energies of the 3 eigenstates relative to -2μ for repulsive (left) and attractive (right) interactions. E_0 is in green, and E_{\pm} are in gold and blue, respectively.

Comments. Evidently, for $N \in \{0, 1, 2\}$, the Bose and Fermi 2-site models behave almost identically. Without spin, however, the Bose state spaces have half the dimension of the Fermi spaces. Indeed, the thermodynamic properties of both systems (see Appendix E) are also identical: spin does not affect the physics at low N . At $N = 2$, the Fermi coupling γ is twice the Bose coupling g . We attribute this to the degeneracy of \uparrow and \downarrow states in the Fermi-Hubbard model, each of which contribute a coupling g . For $N > 2$, however, the bosonic Hubbard model has no Pauli exclusion and allows each site to have higher occupation. We will see that this has important consequences in the many-body case, which we attack next following Philip Anderson's mantra that “more is different” [2].

9.2 Many Bosons

To study the fixed- N model, we return to the Fock space basis $\beta = \{|n_1, n_2\rangle\}$. Subspaces of constant N are constrained by $n_1 + n_2 = N$, so a basis for such a subspace may be written in terms of a single natural number $n \leq N$ labeling the occupation of the first site:

$$\beta_N = \{|0, N\rangle, |1, N-1\rangle, \dots, |N, 0\rangle\} = \{|0\rangle, \dots, |N\rangle\} = \{|n\rangle\}. \quad (9.10)$$

The last two terms of the Bose-Hubbard Hamiltonian (E.14) act diagonally on this basis, producing a function quadratic in both n and N :

$$\begin{aligned} \hat{H}_{U,\mu} |n\rangle &= \left[\frac{U}{2} ((n^2 - n) + (N - n)^2 - (N - N)) - \mu N \right] |N\rangle = \\ &= [U(n^2 - Nn) + c_N] |n\rangle \equiv E_n |n\rangle, \quad c_N(U, \mu) \equiv \frac{U}{2} N^2 - \left(\frac{U}{2} + \mu\right) N. \end{aligned} \quad (9.11)$$

Meanwhile, the t term produces off-diagonal contributions proportional to $|n \pm 1\rangle$. Overall, \hat{H} acts on the fixed- N basis β_N by

$$\hat{H} |n\rangle = -t(|n-1\rangle + |n+1\rangle) + E_n |n\rangle. \quad (9.12)$$

In matrix form, the fixed- N Hamiltonian is an $(N+1) \times (N+1)$ tridiagonal symmetric matrix with E_n along the diagonal and $-t$ along the upper and lower bands:

$$\hat{H}_N = \begin{pmatrix} E_0 & -t & 0 & 0 & \cdots \\ -t & E_1 & -t & 0 & \\ 0 & -t & E_2 & -t & \\ 0 & 0 & -t & \ddots & \ddots \\ \vdots & & & \ddots & \ddots & -t \\ & & & & -t & E_N \end{pmatrix}. \quad (9.13)$$

\hat{H}_N is in principle diagonalizable, but unfortunately no analytic expression for its eigenvalues or eigenvectors exists. Nevertheless, in Appendix F we discuss some partial results towards this goal; there are ultimately more interesting mathematically than physically.

While we cannot diagonalize \hat{H} analytically, we can do so numerically using standard methods under the broad umbrella of “exact diagonalization” [13] [22]. The plots below show the system’s average occupation for $N \leq 10$, which is virtually indistinguishable from the limit $N \rightarrow \infty$. To simulate the system in *Mathematica*:

1. We construct the fixed- N Hamiltonian \hat{H}_N , numerically diagonalize it using sparse matrix methods [29], and obtain its eigenvalues E_α as functions of U , t , and μ .
2. We write down the fixed- N partition function $Z_N = \sum_\alpha e^{-\beta E_\alpha}$.
3. We repeat this procedure in a loop over $N \leq 10$, and compute the many-body partition function $Z = \sum_N Z_N$ and mean occupation number $\langle N \rangle = \frac{1}{Z} \sum_N N Z_N$.
4. We plot $\langle N \rangle$ against (U, μ) and (t, μ) separately.

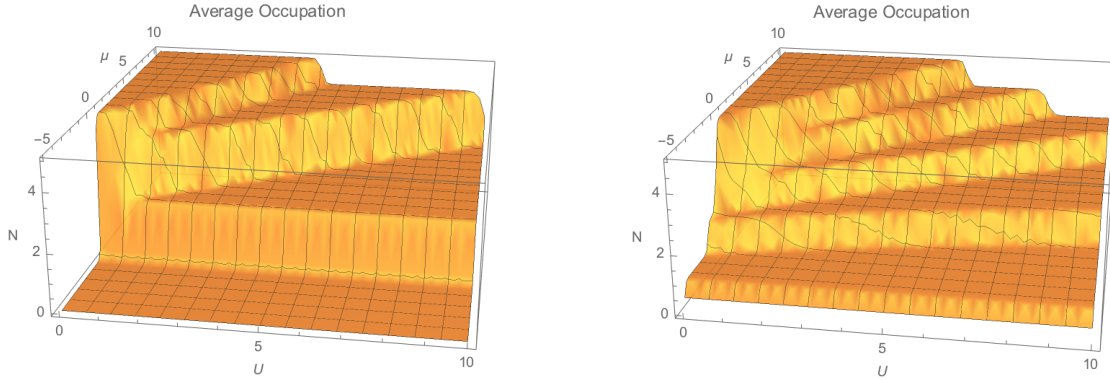


Figure 10: Mean occupation number $N(U, \mu)$ with $t = 0$ (left) and $t = 5$ (right).

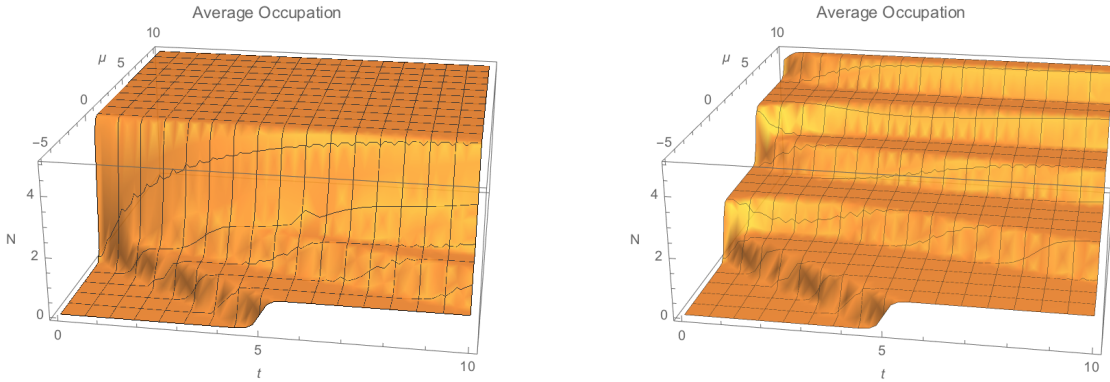


Figure 11: Mean occupation number $N(t, \mu)$ with $U = 0$ (left) and $U = 5$ (right).

The shape of these plots and their physics is familiar from §7, showing that even a 2-site system displays the full gamut of Hubbard behavior. It also shows that t and U terms can coexist rather peacefully without destroying each other's particularities. The main effect of nonzero hopping is to split the plateaus in $N(U, \mu)$ into pairs of similar slope, with energy separation comparable to t ; nonzero U seems to do the same to $N(t, \mu)$. Note also that the plots on the right reproduce the correct limiting behavior of their counterparts on the left.

9.3 High-Temperature Limit

In this section, we present a cute demonstration of the unexpected synergy between mathematics and physics; the result is a computation of the 2-site Bose-Hubbard model's average energy in the high-temperature limit. Observe that $\hat{H}_N = -t\hat{K}_N + \hat{E}_N$, where \hat{K}_N is a tridiagonal matrix with ones along the upper and lower bands and zeros on the main diagonal, and $\hat{E}_N = \text{diag}(E_0, \dots, E_N)$. \hat{E}_N is diagonal, so its eigenvalues are simply E_n . Meanwhile, there is a well-known formula for Toeplitz tridiagonal matrices [19]: in dimension d ,

$$A = \begin{pmatrix} a & b & & & \\ c & a & b & & \\ & c & a & \ddots & \\ & & \ddots & \ddots & b \\ & & & c & a \end{pmatrix} \implies \lambda_k = a + 2\sqrt{bc} \cos\left(\frac{k\pi}{d+1}\right), \quad k \in \{1, \dots, n\}. \quad (9.14)$$

In our case, $a = 0$ and $b = c = 1$, and we have shifted indices $k = n + 1$ and $d = N + 1$. Therefore the spectra of the two components of \hat{H} are

$$\sigma(-t\hat{K}_N) = -2t \cos\left(\frac{(n+1)\pi}{N+2}\right), \quad \sigma(\hat{E}_N) = E_n, \quad n \in \mathbb{N}_{\leq N}. \quad (9.15)$$

The spectrum of $-t\hat{K}_N$ looks oddly like the dispersion relation ε_k from our analysis of the $U = 0$ Hubbard model in §7.2. (Indeed, as $U \rightarrow 0$, \hat{H}_N approaches $-t\hat{K}_N$.) Moreoever, if we interpret the argument $\frac{(n+1)\pi}{N+2}$ as an analog of ka , we see that that the number imbalance of bosons between the two sites directly controls their quasimomentum.

Does this decomposition help us pin down the spectrum of \hat{H}_N ? Unfortunately, eigenvalues of \hat{H}_N are not (as one might expect) sums of the eigenvalues of $-t\hat{K}_N$ and \hat{E}_N unless the summands commute [15]. Unsurprisingly $[\hat{K}_N, \hat{E}_N] \neq 0$, but the entries of the commutator grow only linearly with n , while the entries of \hat{E}_N grow quadratically. In certain regimes, the commutator may thus be regarded as “small,” and we may approximate

$$\lambda_n \approx -2t \cos\left(\frac{(n+1)\pi}{N+2}\right) + E_n. \quad (9.16)$$

In most cases, however, this is a shabby approximation. Instead, we will content ourselves with a weaker result: because matrix traces are additive ($\text{tr}(A + B) = \text{tr } A + \text{tr } B$), the sum of the eigenvalues of \hat{H}_N must match the sums of those of $-t\hat{K}_N$ and \hat{E}_N exactly [15]:

$$\begin{aligned} \sum_{n=0}^N \lambda_{\hat{H}} &= \sum_{n=0}^N (\lambda_{-t\hat{K}} + \lambda_{\hat{E}}) = \sum_{n=0}^N \left[-2t \cos\left(\frac{(n+1)\pi}{N+2}\right) + E_n \right] = \\ &= \sum_{n=0}^N E_n = \frac{U}{3}(N+1)(N^2 - N) - \mu N. \end{aligned} \quad (9.17)$$

Here the cosine sum vanishes by the symmetry of the cosine, and the finite sum over n in E_n was carried out. This sum of eigenvalues is coincidentally related to the average energy in the thermodynamic limit $\beta \rightarrow 0$, where we have

$$\begin{aligned} Z &= \sum_{\alpha} e^{-\beta E_{\alpha}} \longrightarrow \sum_{\alpha} 1 = N+1 \implies \\ E &= \frac{1}{Z} \sum_{\alpha} (E_{\alpha} + \mu N) e^{-\beta E_{\alpha}} \longrightarrow \frac{1}{N+1} \sum_{\alpha} (\lambda_{\hat{H}} + \mu N) = \\ &= \frac{U}{3} \cdot \frac{(N+1)(N^2 - N)}{N+1} = \frac{U}{3}(N^2 - N), \end{aligned} \quad (9.18)$$

depending only on total occupation number and the interaction energy. The fact that t -dependence washes out of E at high energies conversely establishes hopping as a fundamentally low-energy scale: t is a quantum source of energy that is usually small or treated as a perturbation, and competes with U only at large β .

10 Conclusions and Outlook

Conclusions. In this thesis, we have focused mostly on the exact diagonalization, ground state structure, and statistical properties of various tractible limits of the Hubbard model in both its Fermi and Bose incarnations. We began by deriving the Hubbard model as a series of restrictions on a general second-quantized many-body Hamiltonian; we then studied the resulting model’s geometrical and gauge symmetries. We then started toying with its energy scales t and U , eliminating first one and then the other. The $t = 0$ and $U = 0$ Hubbard models behave in remarkably different ways, but rather surprisingly, the statistics of the particle species involved does not qualitatively change the model’s physics in a drastic way.

We then passed to an elementary but exhaustive analysis of the 2-site models, which are exactly diagonalizable and allowed us to freely tune t and U . Our approach took advantage of the conservation of particle number, $[\hat{H}, \hat{N}] = 0$, to break the 2-site problem into manageable subspaces of fixed occupation. Within each sector, we saw again that the Bose and Fermi models behave similarly; this time, however, we got a peek at the interplay of intersite hopping and on-site interactions. Along the way, we came across many interesting mathematical creatures—Jacobi theta functions, tridiagonal matrices, nonlinear recurrence relations, and so on. Broadly speaking, this thesis has been mostly expository; nevertheless, several results related to the Bose-Hubbard model (e.g. its statistical mechanics at $t = 0$ in §7.1, the exact diagonalization carried out in §9.2, and the thermal limit discussed in §9.3) seem to be hitherto missing from the literature.

Outlook. More broadly, this thesis serves as a starting point for the study of many new interesting and nontrivial problems. For instance, any of the following proposals will surely lead into deep waters waiting to be explored:

1. Continue the program of studying the thermodynamical properties of Hubbard models. If we compute the heat capacity of a given system, for example, we can also compute its thermodynamic entropy:

$$C = \frac{dE}{dT} \implies S_{\text{th}} = \int_0^T \frac{C}{T'} dT'. \quad (10.1)$$

We can also compute density matrices for the many-body states we are analyzing, and from there we may find the entanglement entropy $S_{\text{ent}} = -\text{Tr}(\hat{\rho} \log \hat{\rho})$. Comparing the classical and quantum measures of entropy may prove fruitful for revealing more about the Hubbard model’s low-temperature physics.

2. Within the context of 2-site models, a modest generalization of the Hamiltonian might allow for non-homogeneous tunneling or interactions, breaking the geometrical symmetry between the two sites. Physically, this corresponds to allowing a spatially varying trapping potential on the lattice. It might be enlightening to see what happens when one site is preferred over the other, since the model we have studied above is a degenerate case in this regard. As is often the case in physics, studying a generalized scenario often yields up powerful tools that, when applied to the special case of interest, can tell us much more about its physics from a higher perspective.

3. Extend the analysis of few-site models to 3 or 4 sites. In many-body physics, zero, one, or two is “few” while 3 or more is “many;” it is therefore reasonable to expect new and interesting behavior, mostly or fully indicative of the “full” Hubbard model, to arise on these lattices. These models also offer the first glimpse of nontrivial lattice geometries: 3 sites may be arranged as a triangle or as a line (i.e. no tunneling between the edge sites), while 4 sites may appear as a square (commonly called a plaquette) or as a tetrahedron. The literature on these models is scant, and the prospect of adding something new to the corpus of human knowledge is itself a strong motivation.
4. Explore the consequences of modifying lattice geometry. We first broached the importance of geometry by mentioning bipartite lattices in the context of particle-hole symmetry, and we later wondered whether changing the arrangement of a fixed number of lattice sites changes its average filling. In general, changing the connectivity of the lattice strongly affects tunneling, and it would be interesting to look for geometries that extremize quasimomentum, occupation, energy, etc. per lattice site in each dimension.
5. From the perspective of quantum field theory, it is rather boring to study only lattice models: the real excitement starts with a continuum limit. As the intersite spacing shrinks to zero, we may be able to formulate a continuum Hubbard Hamiltonian in the language of quantum field theory. Powerful field-theoretic operator, path-integral, and renormalization-group methods exist to help pin down the ground state of a given model, or at least to analyze its low-energy behavior [17]. One might hope that a “Hubbard field” will yield at least as much insight as the Hubbard lattice already has.
6. The phase diagram of the Hubbard model is an active area of intense research, but not a topic this thesis has directly addressed. Besides the Mott insulating phase, the Hubbard model exhibits superfluidity and antiferromagnetism [28], as well as complex phase transitions between these phases. It would certainly be fruitful to explore these behaviors further within and beyond the limiting cases discussed here.

Part IV

Appendices

Table of Contents

A	The Hubbard Model from Many-Body Theory	41
B	Some Algebraic Results	42
C	Fermi-Hubbard Limits	43
C.1	No Hopping	43
C.2	No Interactions	44
D	Bose-Hubbard Limits	44
D.1	No Hopping	44
D.2	No Interactions	46
E	Two-Site Thermodynamics	47
E.1	Fermi-Hubbard Model	47
E.2	Bose-Hubbard Model	49
F	Tridiagonal Matrices and Recurrences	50

A The Hubbard Model from Many-Body Theory

Substituting the single-band field operators into the full Hamiltonian (3.1) yields

$$\hat{H} = \hat{H}_0 + \hat{H}_{\text{int}} = \quad (\text{A.1})$$

$$= \sum_{\sigma} \int d^3r \hat{\psi}_{\sigma}^{\dagger}(\mathbf{r}) \left[-\frac{\hbar^2}{2m} \nabla^2 + V_{\text{lat}}(\mathbf{r}) + V_{\text{tr}}(\mathbf{r}) \right] \hat{\psi}_{\sigma}(\mathbf{r}) \\ + \frac{g}{2} \sum_{\sigma\sigma'} \int d^3r \hat{\psi}_{\sigma}^{\dagger}(\mathbf{r}) \hat{\psi}_{\sigma'}^{\dagger}(\mathbf{r}) \hat{\psi}_{\sigma'}(\mathbf{r}) \hat{\psi}_{\sigma}(\mathbf{r}) = \quad (\text{A.2})$$

$$= \sum_{\sigma} \int d^3r \left(\sum_i w_i^* \hat{c}_{i\sigma}^{\dagger} \right) \left[-\frac{\hbar^2}{2m} \nabla^2 + V_{\text{lat}} + V_{\text{tr}} \right] \left(\sum_j w_j \hat{c}_{j\sigma} \right) \\ + \frac{g}{2} \sum_{\sigma\sigma'} \int d^3r \left(\sum_i w_i^* \hat{c}_{i\sigma}^{\dagger} \right) \left(\sum_j w_j^* \hat{c}_{j\sigma'}^{\dagger} \right) \left(\sum_k w_k \hat{c}_{k\sigma'} \right) \left(\sum_l w_l \hat{c}_{l\sigma} \right) = \quad (\text{A.3})$$

$$= \sum_{ij,\sigma} \int d^3r w_i^* \left[-\frac{\hbar^2}{2m} \nabla^2 + V_{\text{lat}} \right] w_j \hat{c}_{i\sigma}^{\dagger} \hat{c}_{j\sigma} + \underbrace{\sum_{ij,\sigma} \int d^3r V_{\text{tr}} w_i^* w_j \hat{c}_{i\sigma}^{\dagger} \hat{c}_{j\sigma}}_{(*)} \\ + \frac{g}{2} \sum_{\sigma\sigma'} \sum_{ijkl} \int d^3r w_i^* w_j^* w_k w_l \hat{c}_{i\sigma}^{\dagger} \hat{c}_{j\sigma'}^{\dagger} \hat{c}_{k\sigma'} \hat{c}_{l\sigma} = \quad (\text{A.4})$$

$$= - \sum_{ij,\sigma} t_{ij} \hat{c}_{i\sigma}^{\dagger} \hat{c}_{j\sigma} + \frac{1}{2} \sum_{\sigma\sigma'} \sum_{ijkl} U_{ijkl} \hat{c}_{i\sigma}^{\dagger} \hat{c}_{j\sigma'}^{\dagger} \hat{c}_{k\sigma'} \hat{c}_{l\sigma} + \overbrace{\sum_{i,\sigma} \varepsilon_i \hat{n}_{i\sigma}}^{(*)}. \quad (\text{A.5})$$

In (A.4), we used linearity to move all sums to the left and separated the trapping potential from the other single-particle terms. We then used the fact that V_{tr} does not vary much over a single lattice site in order to consider it a constant with respect to w_j . In (A.5), we reordered the terms and introduced several new objects that require explanation [28].

The first and second of these objects are the tunneling and interaction coefficients:

$$t_{ij} \equiv - \int d^3r w_i^* \left[-\frac{\hbar^2}{2m} \nabla^2 + V_{\text{lat}}(\mathbf{r}) \right] w_j; \quad U_{ijkl} \equiv g \int d^3r w_i^* w_j^* w_k w_l. \quad (\text{A.6})$$

The last term was cooked up using the orthogonality of the Wannier functions:

$$(*) = \sum_{i,\sigma} \sum_j \int d^3r V_{\text{tr}} w_i^* w_j \hat{c}_{i\sigma}^{\dagger} \hat{c}_{j\sigma} = \sum_{i,\sigma} \int d^3r V_{\text{tr}}(\mathbf{r}) |w_i(\mathbf{r})|^2 \hat{c}_{i\sigma}^{\dagger} \hat{c}_{i\sigma} = \\ = \sum_{i,\sigma} V_{\text{tr}}(\mathbf{r}_i) \hat{n}_{i\sigma} \equiv \sum_{i,\sigma} \varepsilon_i \hat{n}_{i\sigma} \implies \varepsilon_i = V_{\text{tr}}(\mathbf{r}_i). \quad (\text{A.7})$$

Since t_{ij} is a kinetic term, we can rewrite it in terms of the Bloch states:

$$\begin{aligned}
 t_{ij} &\equiv -\int d^3r w_i^* \left[-\frac{\hbar^2}{2m} \nabla^2 + V_{\text{lat}}(\mathbf{r}) \right] w_j = \\
 &= -\int d^3r \left(\frac{1}{\sqrt{N}} \sum_{\mathbf{q}} e^{i\mathbf{q} \cdot \mathbf{r}_i} \phi_{\mathbf{q}}^* \right) \left[-\frac{\hbar^2}{2m} \nabla^2 + V_{\text{lat}} \right] \left(\frac{1}{\sqrt{N}} \sum_{\mathbf{q}'} e^{-i\mathbf{q}' \cdot \mathbf{r}_j} \phi_{\mathbf{q}'} \right) = \\
 &= -\frac{1}{N} \sum_{\mathbf{q}\mathbf{q}'} e^{i\mathbf{q} \cdot \mathbf{r}_i} e^{-i\mathbf{q}' \cdot \mathbf{r}_j} \int d^3r \phi_{\mathbf{q}}^* \left[-\frac{\hbar^2}{2m} \nabla^2 + V_{\text{lat}} \right] \phi_{\mathbf{q}'} = \\
 &= -\frac{1}{N} \sum_{\mathbf{q}} e^{i\mathbf{q} \cdot (\mathbf{r}_i - \mathbf{r}_j)} \underbrace{\int d^3r \phi_{\mathbf{q}}^* \left[-\frac{\hbar^2}{2m} \nabla^2 + V_{\text{lat}} \right] \phi_{\mathbf{q}}}_{\varepsilon_{\mathbf{q}}} = -\frac{1}{N} \sum_{\mathbf{q}} \varepsilon_{\mathbf{q}} e^{i\mathbf{q} \cdot (\mathbf{r}_i - \mathbf{r}_j)}. \quad (\text{A.8})
 \end{aligned}$$

Here $\varepsilon_{\mathbf{q}}$ is called the dispersion relation and describes the tight-binding band structure.

B Some Algebraic Results

Proposition B.1. *The Hubbard Hamiltonian $\hat{H} = -t\hat{H}_0 + U\hat{D} - \mu\hat{N}$ commutes with the number operator: $[\hat{H}, \hat{N}] = 0$ for both bosons and fermions.*

Proof. We consider both the Fermi and Bose cases; we must show in each case that

$$[\hat{H}_0, \hat{N}] = [\hat{D}, \hat{N}] = [\hat{N}, \hat{N}] = 0. \quad (\text{B.1})$$

The last equality is trivial, and the second one holds because \hat{D} is composed solely of products of number operators $\hat{n}_{j(\sigma)}$, which all commute with $\hat{N} = \sum_{j(\sigma)} \hat{n}_{j(\sigma)}$. The first commutator vanishes in both the Fermi and Bose cases due to the following elementary lemma [21] [7].

Lemma B.2. *Starting with the fundamental relations (2.5-2.6), it quickly follows that*

$$\begin{aligned}
 [\hat{n}_{j'}, \hat{a}_j^\dagger] &= \hat{a}_{j'}^\dagger \delta_{jj'}, & [\hat{n}_{j'}, \hat{a}_j] &= -\hat{a}_{j'} \delta_{jj'}; \\
 [\hat{n}_{j'\sigma'}, \hat{c}_{j\sigma}^\dagger] &= \hat{c}_{j'\sigma'}^\dagger \delta_{jj'} \delta_{\sigma\sigma'}; & [\hat{n}_{j'\sigma'}, \hat{c}_{j\sigma}] &= -\hat{c}_{j'\sigma'} \delta_{jj'} \delta_{\sigma\sigma'}. \quad (\text{B.2})
 \end{aligned}$$

Using this result, we will show the computation only for the Bose operators, noting that the Fermi case is exactly identical to the one below except for the addition of spin labels.

$$\begin{aligned}
 [\hat{N}, \hat{H}_0] &= \left[\sum_{j'} \hat{n}_{j'}, \sum_{\langle ij \rangle} (\hat{a}_i^\dagger \hat{a}_j + \text{h.c.}) \right] = \sum_{\langle ij \rangle j'} [\hat{n}_{j'}, (\hat{a}_i^\dagger \hat{a}_j + \text{h.c.})] = \\
 &= \sum_{\langle ij \rangle j'} \left([\hat{n}_{j'}, \hat{a}_i^\dagger \hat{a}_j] + \text{h.c.} \right) = \sum_{\langle ij \rangle j'} \left(\hat{a}_i^\dagger [\hat{n}_{j'}, \hat{a}_j] + [\hat{n}_{j'}, \hat{a}_i^\dagger] \hat{a}_j + \text{h.c.} \right) = \\
 &= \sum_{\langle ij \rangle j'} \left(-\hat{a}_i^\dagger \hat{a}_{j'} \delta_{jj'} + \hat{a}_{j'}^\dagger \delta_{ij'} \hat{a}_j + \text{h.c.} \right) = \sum_{\langle ij \rangle} \left(-\hat{a}_i^\dagger \hat{a}_j + \hat{a}_i^\dagger \hat{a}_j + \text{h.c.} \right) = 0. \quad (\text{B.3})
 \end{aligned}$$

Here ‘‘h.c.’’ stands for ‘‘hermitian conjugate,’’ and is used to omit redundant computations and to show that both hopping terms in \hat{H}_0 commute with \hat{N} separately. ■

Proposition B.3. *The operators \hat{S}_i generate a representation of $SU(2)$, and the Hubbard Hamiltonian commutes with all of the \hat{S}_i : $[\hat{S}_i, \hat{H}] = 0$.*

Proof (sketch). We will not prove the first part, but it suffices to show that the S_i , defined by (5.2), form a basis for the fundamental representation of the corresponding Lie algebra $\mathfrak{su}(2)$, i.e. that $[S_\alpha, S_\beta] = i\varepsilon_{\alpha\beta\gamma}S_\gamma$. A short calculation shows that indeed $[\hat{S}_x, \hat{S}_y] = i\hat{S}_z$, and the other cyclic permutations are similar.

Towards the second part, we will show that $[\hat{S}_z, \hat{H}] = 0$; the commutators with \hat{S}_x and \hat{S}_y are similar. To start, observe that $\hat{S}_z = \frac{1}{2}(\hat{N}_\uparrow - \hat{N}_\downarrow)$. The fact that \hat{S}_z is expressed as a sum of number operators kills its commutators with \hat{N} and \hat{D} as argued above in the proposition above, so what remains is the commutator

$$[\hat{S}_z, \hat{H}_0] = \frac{1}{2}([\hat{N}_\uparrow, \hat{H}_0] - [\hat{N}_\downarrow, \hat{H}_0]) = \frac{1}{2}(0 - 0) = 0. \quad (\text{B.4})$$

Both terms vanish due to the proof of the result above, which shows that number operators (in particular, those counting spins) commute with \hat{H}_0 .

For more detail, see [8]. ■

C Fermi-Hubbard Limits

C.1 No Hopping

The one-site Hamiltonian is $\hat{H} = U(\hat{n}_{j\uparrow}\hat{n}_{j\downarrow}) - \mu(\hat{n}_{j\uparrow} + \hat{n}_{j\downarrow})$. The basis states and energies are

$$\hat{H}|0\rangle = 0; \quad \hat{H}|\downarrow\rangle = -\mu|\downarrow\rangle; \quad \hat{H}|\uparrow\rangle = -\mu|\uparrow\rangle; \quad \hat{H}|2\rangle = (U - 2\mu)|2\rangle. \quad (\text{C.1})$$

We label by A_α the energy eigenvalues of operator \hat{A} in energy eigenstate $|\alpha\rangle$. The partition function, average energy, and average occupation are [24]

$$Z(\beta) = \sum_{\alpha \in \{0, \downarrow, \uparrow, 2\}} e^{-\beta E_\alpha} = 1 + 2e^{\beta\mu} + e^{2\beta\mu - \beta U}. \quad (\text{C.2})$$

$$E = \frac{1}{Z} \sum_{\alpha} (UD_\alpha)e^{-\beta E_\alpha} = \frac{Ue^{2\beta\mu - \beta U}}{1 + 2e^{\beta\mu} + e^{2\beta\mu - \beta U}}. \quad (\text{C.3})$$

$$N = \frac{1}{Z} \sum_{\alpha} N_\alpha e^{-\beta E_\alpha} = \frac{2(e^{\beta\mu} + e^{2\beta\mu - \beta U})}{1 + 2e^{\beta\mu} + e^{2\beta\mu - \beta U}}. \quad (\text{C.4})$$

C.2 No Interactions

We substitute the momentum-space creation and annihilation operators into the tight-binding Hamiltonian (6.4). For shorthand, we set $\mathbf{r}_j \rightarrow j$ and $\mathbf{q}_k \rightarrow k$, with jk understood as $\mathbf{r}_k \cdot \mathbf{q}_k$ and $a \equiv j - j'$ as the lattice vector $\mathbf{a} = \mathbf{r}_j - \mathbf{r}_{j'}$. Following [24], we find that

$$\begin{aligned}
\hat{H} &= -t \sum_{\langle jj' \rangle, \sigma} (\hat{c}_{j\sigma}^\dagger \hat{c}_{j'\sigma} + \hat{c}_{j'\sigma}^\dagger \hat{c}_{j\sigma}) - \mu \sum_{j, \sigma} \hat{c}_{j\sigma}^\dagger \hat{c}_{j\sigma} = \\
&= -\frac{t}{M} \sum_{\langle jj' \rangle, \sigma} \left[\left(\sum_k e^{-ijk} \hat{c}_{k\sigma}^\dagger \right) \left(\sum_k e^{ij'k} \hat{c}_{k\sigma} \right) + \left(\sum_k e^{-ij'k} \hat{c}_{k\sigma}^\dagger \right) \left(\sum_k e^{ijk} \hat{c}_{k\sigma} \right) \right] - \\
&\quad - \frac{\mu}{M} \sum_{j, \sigma} \left[\left(\sum_k e^{-ijk} \hat{c}_{k\sigma}^\dagger \right) \left(\sum_k e^{ijk} \hat{c}_{k\sigma} \right) \right] = \\
&= -\frac{t}{M} \sum_{\langle jj' \rangle} \sum_{k, \sigma} \left(e^{-ijk} e^{ij'k} + e^{ijk} e^{-ij'k} \right) \hat{c}_{k\sigma}^\dagger \hat{c}_{k\sigma} - \frac{\mu}{M} \sum_{j, k, \sigma} e^{-ijk} e^{ijk} \hat{c}_{k\sigma}^\dagger \hat{c}_{k\sigma} = \\
&= -\frac{t}{M} \sum_{\langle jj' \rangle} \sum_{k, \sigma} \left(e^{-ik(j-j')} + e^{ik(j-j')} \right) \hat{n}_{k\sigma} - \frac{\mu}{M} \sum_{j, k, \sigma} \hat{n}_{k\sigma} = \\
&= -\sum_{k, \sigma} \left(2t \cos(ka) + \mu \right) \hat{n}_{k\sigma} = \sum_{k, \sigma} (\varepsilon_k - \mu) \hat{n}_{k\sigma}, \quad \varepsilon_k = -2t \cos(ka). \tag{C.5}
\end{aligned}$$

For simplicity, have used the index k to label all momentum expansions; more care would have resulted in pages of delta function expansions. On the last line, we recognized $e^{ika} + e^{-ika} = 2 \cos(ka)$, performed the sum over $\langle jj' \rangle$ to get rid of M , and finally grouped the t and μ terms together to obtain the result.

The Hamiltonian for a single momentum mode is $\hat{H} = (\varepsilon_k - \mu) \hat{n}_k$; the partition function, average energy, and average occupation number are given by

$$Z(\beta) = \sum_{\alpha} e^{-\beta E_{\alpha}} = 1 + 2e^{-\beta(\varepsilon_k - \mu)} + e^{-2\beta(\varepsilon_k - \mu)} = \left(1 + e^{\beta(2t+\mu)} \right)^2; \tag{C.6}$$

$$N = \langle \hat{n}_k \rangle = \frac{2(e^{-\beta(\varepsilon_k - \mu)} + e^{-2\beta(\varepsilon_k - \mu)})}{1 + 2e^{-\beta(\varepsilon_k - \mu)} + e^{-2\beta(\varepsilon_k - \mu)}} = \frac{2}{1 + e^{\beta(\varepsilon_k - \mu)}}; \tag{C.7}$$

$$E = \varepsilon_k \langle \hat{n}_k \rangle = \frac{2\varepsilon_k (e^{-\beta(\varepsilon_k - \mu)} + e^{-2\beta(\varepsilon_k - \mu)})}{1 + 2e^{-\beta(\varepsilon_k - \mu)} + e^{-2\beta(\varepsilon_k - \mu)}} = \frac{2\varepsilon_k}{1 + e^{\beta(\varepsilon_k - \mu)}}. \tag{C.8}$$

D Bose-Hubbard Limits

D.1 No Hopping

The one-site Hamiltonian is $\hat{H} = \frac{U}{2} \hat{n}(\hat{n} - 1) - \mu \hat{n}$. The basis states and their energies are

$$\hat{H} |n\rangle = \left[\frac{U}{2} n(n-1) - \mu n \right] |n\rangle \implies E(n) = \frac{U}{2} n^2 - \left(\frac{U}{2} + \mu \right) n. \tag{D.1}$$

The partition function is

$$\begin{aligned} Z(\beta) &= \sum_{n \in \mathbb{N}} e^{-\beta E(n)} = \sum_{n \in \mathbb{N}} \exp \left[-\beta \frac{U}{2} n^2 + \beta \left(\frac{U}{2} + \mu \right) n \right] = \\ &= \sum_{n \in \mathbb{N}} \left[\exp \left(-\frac{\beta U}{2} \right) \right]^{n^2} \left[\exp \left(\frac{\beta U}{2} + \beta \mu \right) \right]^n. \end{aligned} \quad (\text{D.2})$$

This series looks strikingly like the Jacobi theta function [20], defined and denoted by

$$\begin{aligned} \vartheta(z, \tau) &= \sum_{n \in \mathbb{Z}} \exp (\pi i n^2 \tau + 2\pi i n z) = \sum_{n \in \mathbb{Z}} (e^{\pi i \tau})^{n^2} (e^{2\pi i z})^n = \\ &= \sum_{n \in \mathbb{Z}} q^{n^2} w^n = \vartheta(w, q) = \vartheta(z, q). \end{aligned} \quad (\text{D.3})$$

Our partition function takes almost the same form after setting

$$q = e^{-\beta U/2}; \quad 2\pi i z = \beta \left(\frac{U}{2} + \mu \right) \implies z = -\frac{i\beta}{2\pi} \left(\frac{U}{2} + \mu \right). \quad (\text{D.4})$$

Then the only difference between $Z(\beta)$ and $\vartheta(z, q)$ is that Z sums over natural numbers (occupations), whereas ϑ sums over all integers. If we entertain the possibility of negative occupation numbers [18] (holes in a Bose sea of sorts, but not antiparticles), which notably does not ruin the boundedness of the excitation spectrum, then we obtain

$$Z_*(\beta) = \sum_{n \in \mathbb{Z}} \left(e^{-\beta U/2} \right)^{n^2} \left[\exp \left(\frac{\beta U}{2} + \beta \mu \right) \right]^n = \vartheta \left(-\frac{i\beta}{2\pi} \left(\frac{U}{2} + \mu \right), e^{-\beta U/2} \right). \quad (\text{D.5})$$

We can approximate our way to a closed-form expression for Z_* . Notice that for $U > 0$, each term $e^{-\beta E(n)}$ is a Gaussian in n ; this suggests the replacement of the sum with an integral:

$$Z_* \rightarrow \int_{\mathbb{R}} dn \exp \left[-\frac{\beta U}{2} n^2 + \beta \left(\frac{U}{2} + \mu \right) n \right] = \sqrt{\frac{2\pi}{\beta U}} e^{\frac{\beta(U+2\mu)^2}{8U}} = \sqrt{\frac{2\pi}{\beta U}} e^{-\beta E_0}, \quad (\text{D.6})$$

where E_0 is the ground state energy (7.4). However, we must note that this approximation is only very accurate at high temperatures $\beta \rightarrow 0$, where many terms in the original sum contribute appreciably to Z_* to model a ‘gentle’ function of n .

If we do not allow $n \leq 0$, we can still write an exact(-ish), but rather unwieldy, expression for Z . The parabola $E(n)$ is symmetric about n_0 , so the tail of the partition function summing over occupations $n \geq n_0$ is (about) half the value of the theta function: therefore the “physical” partition function Z is written in terms of the “more natural” Z_* as

$$\sum_{n=n_0}^{\infty} e^{-\beta E(n)} = \frac{1}{2} Z_*(\beta) \implies Z(\beta) = \sum_{n \in \mathbb{N}} q^{n^2} w^n = \frac{1}{2} Z_*(\beta) + \sum_{n=0}^{n_0} e^{-\beta E_n}. \quad (\text{D.7})$$

When $E(n)$ is deep and narrow due to a large U , the energies for $0 \leq n \leq n_0$ are strongly negative, making their contributions $e^{-\beta E(n)}$ to the second term in Z negligible: therefore $Z \simeq \frac{1}{2}Z_*$. We may also consider certain special cases. We have:

$$U = 0 \implies Z = \sum_{n \in \mathbb{N}} \exp(\beta\mu)^n = \frac{1}{1 - e^{\beta\mu}}, \quad (\text{D.8})$$

$$\mu = -\frac{U}{2} \implies Z = \sum_{n \in \mathbb{N}} \exp\left(-\frac{\beta U}{2}\right)^{n^2} = \frac{1}{2}\vartheta(0, e^{-\beta U/2}). \quad (\text{D.9})$$

Next, we compute the average energy and occupation number:

$$\begin{aligned} N &= \frac{1}{Z} \sum_{n \in \mathbb{N}} n e^{-\beta E(n)}; & E &= \frac{U}{2} \langle \hat{n}(\hat{n}-1) \rangle = \frac{U}{2Z} \sum_{n \in \mathbb{N}} n(n-1) e^{-\beta E(n)} = \\ & & &= \frac{U}{2Z} \sum_{n \in \mathbb{N}} n^2 e^{-\beta E(n)} - N. \end{aligned} \quad (\text{D.10})$$

Unfortunately, there is no closed-form expression for these sums, but they are still amenable to high-temperature integral approximations. Passing to the “complete” sums over \mathbb{Z} , we have expressions resembling path-integral calculations of correlation functions:

$$\begin{aligned} N_* &\longrightarrow \frac{1}{Z_*} \int_{\mathbb{R}} dn n \exp\left[-\frac{\beta U}{2}n^2 + \beta\left(\frac{U}{2} + \mu\right)n\right] = \\ &= \frac{1}{Z_*} \sqrt{\frac{\pi}{2\beta U^3}} (U + 2\mu) e^{-\beta E_0} = \frac{U + 2\mu}{2U}; \end{aligned} \quad (\text{D.11})$$

$$\begin{aligned} E_* &\longrightarrow \frac{U}{2Z_*} \int_{\mathbb{R}} dn n^2 \exp\left[-\frac{\beta U}{2}n^2 + \beta\left(\frac{U}{2} + \mu\right)n\right] - N = \\ &= \frac{1}{Z_*} \sqrt{\frac{\pi}{2\beta^3 U^5}} \left(U(4 + \beta U) + 4\beta\mu U + 4\beta\mu^2\right) e^{-\beta E_0} - \frac{U + 2\mu}{2U} = \\ &= \frac{1}{2U} \left(\frac{U(4 + \beta U) + 4\beta\mu U + 4\beta\mu^2}{\beta U} - (U + 2\mu)\right). \end{aligned} \quad (\text{D.12})$$

We could have tried to compute E as the logarithmic derivative of Z ; towards this goal, [9] gives a series representation for $\frac{\vartheta'}{\vartheta}$. Unfortunately, this representation is messy and less likely to yield an expression in elementary functions than what we have written above.

D.2 No Interactions

The single-mode Hamiltonian is $\hat{H} = (\varepsilon_k - \mu)\hat{n}$. The partition function is

$$Z(\beta) = \sum_{n \in \mathbb{N}} \exp[-\beta(\varepsilon_k - \mu)n] = \frac{1}{1 - e^{-\beta(\varepsilon_k - \mu)}}. \quad (\text{D.13})$$

The average energy and particle number are

$$\begin{aligned} N &= \frac{1}{Z} \sum_{n \in \mathbb{N}} n e^{-\beta(\varepsilon_k - \mu)n} = \frac{(1 - e^{-\beta(\varepsilon_k - \mu)})e^{-\beta(\varepsilon_k - \mu)}}{(1 - e^{-\beta(\varepsilon_k - \mu)})^2} = \\ &= \frac{1}{e^{\beta(\varepsilon_k - \mu)} - 1}; & E &= \varepsilon_k N = \frac{\varepsilon_k}{e^{\beta(\varepsilon_k - \mu)} - 1}. \end{aligned} \quad (\text{D.14})$$

E Two-Site Thermodynamics

E.1 Fermi-Hubbard Model

The Hamiltonian (8.1) is

$$\begin{aligned}\hat{H}_F^{(2)} &= -t(\hat{c}_{1\uparrow}^\dagger \hat{c}_{2\uparrow} + \hat{c}_{1\downarrow}^\dagger \hat{c}_{2\downarrow} + \hat{c}_{2\uparrow}^\dagger \hat{c}_{1\uparrow} + \hat{c}_{2\downarrow}^\dagger \hat{c}_{1\downarrow}) + \\ &\quad + U(\hat{n}_{1\uparrow} \hat{n}_{1\downarrow} + \hat{n}_{2\uparrow} \hat{n}_{2\downarrow}) - \mu(\hat{n}_{1\uparrow} + \hat{n}_{1\downarrow} + \hat{n}_{2\uparrow} + \hat{n}_{2\downarrow}) = \\ &= -t(\hat{c}_1^\dagger \hat{c}_2 + \hat{c}_2^\dagger \hat{c}_1) + U\hat{D} - \mu\hat{N}.\end{aligned}\quad (\text{E.1})$$

($N = 0$) The only basis state, $|0\rangle$, has zero energy. Therefore Z and E are

$$Z_0(\beta) = \sum_{\alpha} e^{-\beta E_{\alpha}} = 1; \quad E_0 = \frac{1}{Z} \sum_{\alpha} E_{\alpha} e^{-\beta E_{\alpha}} = 0. \quad (\text{E.2})$$

($N = 1$) The 4 basis states are each doubly degenerate, and have energies $\pm t - \mu$. We have

$$Z_1(\beta) = \sum_{\alpha} e^{-\beta E_{\alpha}} = 2(e^{-\beta(-t-\mu)} + e^{-\beta(t-\mu)}) = 4e^{\beta\mu} \cosh(\beta t); \quad (\text{E.3})$$

$$\begin{aligned}E_1 &= \frac{1}{Z} \sum_{\alpha} (E_{\alpha} + \mu) e^{-\beta E_{\alpha}} = \frac{1}{4} e^{-\beta\mu} \operatorname{sech}(\beta t) \cdot 2e^{\beta\mu} [-te^{\beta t} + te^{-\beta t}] = \\ &= -\frac{1}{2} \operatorname{sech}(\beta t) \cdot 2t \sinh(\beta t) = -t \tanh(\beta t).\end{aligned}\quad (\text{E.4})$$

($N = 2$) There are six eigenstates. Three of them have energy -2μ , one has energy $U - 2\mu$, and the remaining two have energy $2(t\phi_{\pm}(\gamma) - \mu)$ [28]. Here $\gamma \equiv \frac{U}{4t}$ is the dimensionless coupling strength, and $\phi_{\pm}(\gamma) = \gamma \pm \sqrt{1 + \gamma^2} = \gamma \pm \Gamma$, where we have introduced $\Gamma \equiv \sqrt{1 + \gamma^2}$ for shorthand. Then the partition function and average energy are

$$\begin{aligned}Z_2(\beta) &= \sum_{\alpha} e^{-\beta E_{\alpha}} = 3e^{2\beta\mu} + e^{-\beta(U-2\mu)} + e^{-2\beta(t\phi_{+}-\mu)} + e^{-2\beta(t\phi_{-}-\mu)} = \\ &= e^{2\beta\mu} [3 + e^{-\beta U} + 2e^{-2\beta\gamma t} \cosh(2\beta\Gamma t)];\end{aligned}\quad (\text{E.5})$$

$$\begin{aligned}E_2 &= \frac{1}{Z} \sum_{\alpha} (E_{\alpha} + 2\mu) e^{-\beta E_{\alpha}} = \frac{1}{Z} [Ue^{-\beta(U-2\mu)} + 2t\phi_{+}e^{-2\beta(t\phi_{+}-\mu)} + 2t\phi_{-}e^{-2\beta(t\phi_{-}-\mu)}] = \\ &= \frac{e^{2\beta\mu} [Ue^{-\beta U} + 2te^{-2\beta\gamma t} (\phi_{+}e^{2\beta\Gamma t} + \phi_{-}e^{-2\beta\Gamma t})]}{e^{2\beta\mu} [3 + e^{-\beta U} + 2e^{-2\beta\gamma t} \cosh(2\beta\Gamma t)]} = \\ &= \frac{Ue^{-\beta U} + 2te^{-2\beta\gamma t} \cosh(2\beta\Gamma t) (\gamma + \Gamma \tanh(2\beta\Gamma t))}{3 + e^{-\beta U} + 2e^{-2\beta\gamma t} \cosh(2\beta\Gamma t)}.\end{aligned}\quad (\text{E.6})$$

($N = 3$) Much like the case $N = 1$, the four basis states are each doubly degenerate. They have energies $\pm t + (U - 3\mu)$, so the partition function and average energy are

$$Z_3(\beta) = \sum_{\alpha} e^{-\beta E_{\alpha}} = 2(e^{-\beta(-t+(U-3\mu))} + e^{-\beta(t+(U-3\mu))}) = 4e^{-\beta(U-3\mu)} \cosh(\beta t); \quad (\text{E.7})$$

$$\begin{aligned} E_3 &= \frac{1}{Z} \sum_{\alpha} (E_{\alpha} + 3\mu) e^{-\beta E_{\alpha}} = \frac{1}{4} e^{\beta(U-3\mu)} \operatorname{sech}(\beta t) \cdot 2e^{-\beta(U-3\mu)} [(-t+U)e^{\beta t} + (t+U)e^{-\beta t}] = \\ &= \frac{1}{2} \operatorname{sech}(\beta t) \cdot 2[U \cosh(\beta t) - t \sinh(\beta t)] = U - t \tanh(\beta t). \end{aligned} \quad (\text{E.8})$$

($N = 4$) The only basis state, $|22\rangle$, has energy $\hat{H}|22\rangle = (2U - 4\mu)|22\rangle$. The partition function and average energy are therefore

$$Z_4(\beta) = \sum_{\alpha} e^{-\beta E_{\alpha}} = e^{-2\beta(U-2\mu)}; \quad (\text{E.9})$$

$$E_4 = \frac{1}{Z} \sum_{\alpha} (E_{\alpha} + 4\mu) e^{-\beta E_{\alpha}} = e^{2\beta(U-2\mu)} \cdot 2U e^{-\beta(U-2\mu)} = 2U. \quad (\text{E.10})$$

Full treatment. The full partition function for the 2-site Fermi-Hubbard model is

$$\begin{aligned} Z &= Z_0 + Z_1 + Z_2 + Z_3 + Z_4 = \\ &= 1 + 4e^{\beta\mu} \cosh(\beta t) + e^{2\beta\mu} [3 + e^{-\beta U} + 2e^{-2\beta\gamma t} \cosh \Gamma] + \\ &\quad + 4e^{-\beta(U-3\mu)} \cosh(\beta t) + e^{-2\beta(U-2\mu)} = \\ &= 1 + 4e^{\beta\mu} \cosh(\beta t) [1 + e^{-\beta(U-2\mu)}] + \\ &\quad + e^{-2\beta(U-2\mu)} + e^{2\beta\mu} [3 + e^{-\beta U} + 2e^{-2\beta\gamma t} \cosh \Gamma] = \\ &= (1 + e^{-\beta(U-2\mu)}) (1 + 4e^{\beta\mu} \cosh(\beta t)) + e^{2\beta\mu} [3 + 2e^{-2\beta\gamma t} \cosh \Gamma]. \end{aligned} \quad (\text{E.11})$$

The average occupation number is given by

$$N = \frac{1}{Z} \sum_{\alpha} N_{\alpha} e^{-\beta E_{\alpha}} = \frac{1}{Z} \sum_{n=0}^4 n Z_n = \frac{Z_1 + 2Z_2 + 3Z_3 + 4Z_4}{Z_0 + Z_1 + Z_2 + Z_3 + Z_4}. \quad (\text{E.12})$$

We can see from the computations above that this expression will not simplify nicely, so we spare the reader the abject horror of staring it in the face. The average energy

$$E = \sum_{\alpha} (E_{\alpha} + \mu N_{\alpha}) e^{-\beta E_{\alpha}} = \frac{\partial}{\partial \beta} (\log Z) \quad (\text{E.13})$$

meets a similar fate, but rest assured that an exact expression does exist.

E.2 Bose-Hubbard Model

The Hamiltonian (E.14) is

$$\hat{H}_B^{(2)} = -t(\hat{a}_1^\dagger \hat{a}_2 + \hat{a}_2^\dagger \hat{a}_1) + \frac{U}{2}(\hat{n}_1(\hat{n}_1 - 1) + \hat{n}_2(\hat{n}_2 - 1)) - \mu(\hat{n}_1 + \hat{n}_2). \quad (\text{E.14})$$

($N = 0$) The only basis state, $|0\rangle$, has zero energy. Therefore Z and E are

$$Z_0(\beta) = \sum_{\alpha} e^{-\beta E_{\alpha}} = 1; \quad E_0 = \frac{1}{Z} \sum_{\alpha} E_{\alpha} e^{-\beta E_{\alpha}} = 0. \quad (\text{E.15})$$

($N = 1$) The two basis states $|\psi_{\pm}\rangle$ have energies $\pm t - \mu$, so the results for Z and E are almost identical to the Fermi case:

$$Z_1(\beta) = \sum_{\alpha} e^{-\beta E_{\alpha}} = e^{-\beta(-t-\mu)} + e^{-\beta(t-\mu)} = 2e^{\beta\mu} \cosh(\beta t); \quad (\text{E.16})$$

$$\begin{aligned} E_1 &= \frac{1}{Z} \sum_{\alpha} (E_{\alpha} + \mu) e^{-\beta E_{\alpha}} = \\ &= \frac{1}{2} e^{-\beta\mu} \operatorname{sech}(\beta t) \cdot e^{\beta\mu} [-te^{-\beta t} + te^{-\beta t}] = -t \tanh(\beta t). \end{aligned} \quad (\text{E.17})$$

($N = 2$) The three eigenstates have energy $U - 2\mu$ and $tf_{\pm}(g) - 2\mu$ [28], where $g = U/2t$ is the coupling and $f_{\pm} = g + \sqrt{2 + g^2} = g \pm G$, and $G \equiv \sqrt{2 + g^2}$. Then Z and E are

$$\begin{aligned} Z_2(\beta) &= \sum_{\alpha} e^{-\beta E_{\alpha}} = e^{-\beta(U-2\mu)} + e^{-\beta(tf_{+}-2\mu)} + e^{-\beta(tf_{-}-2\mu)} = \\ &= e^{2\beta\mu} [e^{-\beta U} + e^{-\beta gt} \cosh(\beta Gt)]; \end{aligned} \quad (\text{E.18})$$

$$\begin{aligned} E_2 &= \frac{1}{Z} \sum_{\alpha} (E_{\alpha} + 2\mu) e^{-\beta E_{\alpha}} = \frac{1}{Z} [Ue^{-\beta(U-2\mu)} + tf_{+}e^{-\beta(tf_{+}-2\mu)} + tf_{-}e^{-\beta(tf_{-}-2\mu)}] = \\ &= \frac{e^{2\beta\mu} [Ue^{-\beta U} + te^{-\beta gt} (f_{+}e^{\beta Gt} + f_{-}e^{-\beta Gt})]}{e^{2\beta\mu} [e^{-\beta U} + e^{-\beta gt} \cosh(\beta Gt)]} = \\ &= \frac{Ue^{-\beta U} + te^{-\beta gt} \cosh(\beta Gt)(g + G \tanh(\beta Gt))}{e^{-\beta U} + e^{-\beta gt} \cosh(\beta Gt)}. \end{aligned} \quad (\text{E.19})$$

F Tridiagonal Matrices and Recurrences

Consider the symmetric tridiagonal matrix $H_N \in \mathcal{M}_{N+1}(\mathbb{R})$ given by

$$\hat{H}_N = \begin{pmatrix} E_0 & -t & 0 & 0 & \cdots \\ -t & E_1 & -t & 0 & \\ 0 & -t & E_2 & -t & \\ 0 & 0 & -t & \ddots & \ddots \\ \vdots & & & \ddots & \ddots & -t \\ & & & & -t & E_N \end{pmatrix}, \quad \begin{aligned} E_n &= U(n^2 - Nn) + c_N, \\ c_N(U, \mu) &= \frac{U}{2}N^2 - \left(\frac{U}{2} + \mu\right)N, \\ U, t, \mu &\in \mathbb{R}. \end{aligned} \quad (\text{F.1})$$

We aim to diagonalize \hat{H}_N in order to obtain its eigenvalues and eigenvectors.

The most basic approach to our problem begins by considering the characteristic polynomial $\det(\hat{H}_N - \lambda \mathbf{1}_{N+1})$, whose roots $\lambda_0, \dots, \lambda_N$ are the eigenvalues of \hat{H}_N . To this end, define $M_N \equiv \hat{H}_N - \lambda \mathbf{1}_{N+1}$, the tridiagonal matrix with $E_n - \lambda$ along the main diagonal. Naïvely, we can compute $\det M_N$ using expansion by minors: starting from the bottom right, we have

$$\begin{aligned} \det M_N &= (E_N - \lambda) \det(M_{N-1}) + t \begin{vmatrix} M_{N-2} & \mathbf{0} \\ \mathbf{0} & -t \end{vmatrix} + 0 \implies \\ \det M_n &= (E_n - \lambda) \det(M_{n-1}) - t^2 \det(M_{n-2}), \\ \det M_0 &= c_N - \lambda, \quad \det M_1 = (E_1 - \lambda)(c_N - \lambda) - t^2, \end{aligned} \quad (\text{F.2})$$

where we have used $E_0 = E_N = c_N$ in the last line. This defines a nonlinear second-order recurrence relation for the characteristic polynomial of \hat{H} . We may bring it to a generic form by defining $a_n \equiv \det M_n$ and $b_n \equiv E_n - \lambda$:

$$\begin{cases} a_n = b_n a_{n-1} - t^2 a_{n-2}, \\ a_0 = b_0, \quad a_1 = b_0 b_1 - t^2. \end{cases}$$

This is as far as we can go analytically: there is sadly no closed-form solution for a_N .

There is, however, another way to attack the problem: we may use the fact that elementary row operations modify the determinant of a matrix in a controlled manner to massage M_N into a diagonal matrix, from which we can read off its determinant as the product of the diagonal entries. In fact, the only row operation we will need is the addition of scalar multiples of one row or column to another; this leaves the determinant invariant because it only amounts to changing the basis of the matrix [13]. To “diagonalize” M_N , we add $t/(E_{n-1} - \lambda)$ to the n th row and column, with the convention that $n - 1 = 0$ when $n = 0$. Then the following sequence of operations preserves $\det M_N$:

$$\begin{aligned}
 M_N &= \begin{pmatrix} b_0 & -t & & & \\ -t & b_1 & -t & & \\ & -t & b_2 & -t & \\ & & -t & \ddots & -t \\ & & & -t & b_N \end{pmatrix} \sim \begin{pmatrix} b_0 & -t & & & \\ 0 & b_1 - \frac{t^2}{b_0} & -t & & \\ & -t & b_2 & -t & \\ & & -t & \ddots & -t \\ & & & -t & b_N \end{pmatrix} \sim \\
 &\sim \begin{pmatrix} b_0 & 0 & & & \\ 0 & b_1 - \frac{t^2}{b_0} & -t & & \\ & -t & b_2 & -t & \\ & & -t & \ddots & -t \\ & & & -t & b_N \end{pmatrix} \equiv \begin{pmatrix} b'_0 & 0 & & & \\ 0 & b'_1 & -t & & \\ & -t & b_2 & -t & \\ & & -t & \ddots & -t \\ & & & -t & b_N \end{pmatrix} \sim \\
 &\sim \begin{pmatrix} b'_0 & 0 & & & \\ 0 & b'_1 & 0 & & \\ 0 & b'_2 & -t & & \\ & -t & \ddots & -t \\ & & -t & b_N \end{pmatrix} \sim \dots \sim \begin{pmatrix} b'_0 & 0 & & & \\ 0 & b'_1 & 0 & & \\ 0 & b'_2 & 0 & & \\ & 0 & \ddots & 0 & \\ & 0 & & b'_N & \end{pmatrix} = M'_N. \quad (\text{F.3})
 \end{aligned}$$

Here we have introduced the modified diagonal entries b'_n , which satisfy

$$b'_n = b_n - \frac{t^2}{b'_{n-1}}, \quad b'_0 = b_0. \quad (\text{F.4})$$

This is a new recurrence relation—still nonlinear, but now of first order! The “exact” form of each b'_n is given by the (finite) continued fraction

$$\begin{aligned}
 b'_n = b_n - \frac{t^2}{b_{n-1} - \frac{t^2}{b_{n-2} - \frac{t^2}{\ddots - \frac{t^2}{b_1 - \frac{t^2}{b_0}}}}}, \quad b_n = E_n - \lambda. \quad (\text{F.5})
 \end{aligned}$$

Formally, the desired determinant is the polynomial $\det M_N = \prod_{n=0}^N b'_n$, and its roots λ are the energy eigenvalues of \hat{H}_N . Since $\det M_N$ is expressed as a product, its zeros must satisfy

$$b'_n = b_n - \frac{t^2}{b'_{n-1}} = 0 \implies b_n = \frac{t^2}{b'_{n-1}} \iff b'_{n-1} = \frac{t^2}{b_n}. \quad (\text{F.6})$$

Unfortunately this too is a dead end: solving the above entails expanding out the continued fraction b'_{n-1} and solving for λ , a procedure for which there is no exact solution.

References

- [1] The hubbard model at half a century. *Nature Physics*, 9, September 2013.
- [2] Philip W Anderson. More is different. *Science*, 177(4047):393–396, 1972.
- [3] Neil W Ashcroft and N David Mermin. *Solid State Physics*. Saunders College, 1976.
- [4] Assa Auerbach. *Interacting Electrons and Quantum Magnetism*. Springer Science & Business Media, 1994.
- [5] Thomas Busch, Berthold-Georg Englert, Kazimierz Rzażewski, and Martin Wilkens. Two cold atoms in a harmonic trap. *Foundations of Physics*, 28(4):549–559, 1998.
- [6] GS Canright and Steven M Girvin. Fractional statistics: Quantum possibilities in two dimensions. *Science*, 247(4947):1197–1205, 1990.
- [7] Piers Coleman. *Introduction to Many-Body Physics*. Cambridge University Press, 2015.
- [8] Fabian HL Essler, Holger Frahm, Frank Göhmann, Andreas Klümper, and Vladimir E Korepin. *The One-Dimensional Hubbard Model*. Cambridge University Press, 2005.
- [9] Markus Faulhuber. Properties of logarithmic derivatives of jacobi’s theta functions on a logarithmic scale. *arXiv:1709.06006*, 2017.
- [10] Christopher J Foot. *Atomic Physics*, volume 7. Oxford University Press, 2005.
- [11] Markus Greiner, Olaf Mandel, Tilman Esslinger, Theodor W Hänsch, and Immanuel Bloch. Quantum phase transition from a superfluid to a mott insulator in a gas of ultracold atoms. *Nature*, 415(6867), 2002.
- [12] John Hubbard. Electron correlations in narrow energy bands. *Proceedings of the Royal Society of London. Series A. Mathematical and Physical Sciences*, 276(1365):238–257, 1963.
- [13] S Akbar Jafari. Introduction to hubbard model and exact diagonalization. *arXiv:0807.4878*, 2008.
- [14] Robert Jördens, Niels Strohmaier, Kenneth Günter, Henning Moritz, and Tilman Esslinger. A mott insulator of fermionic atoms in an optical lattice. *Nature*, 455(7210), 2008.
- [15] Allen Knutson and Terence Tao. Honeycombs and sums of hermitian matrices. *Notices Amer. Math. Soc*, 48(2), 2001.
- [16] Lev Davidovich Landau and Evgenii Mikhailovich Lifshitz. *Quantum Mechanics: Non-Relativistic Theory*, volume 3. Elsevier, 3rd edition edition, 2013.

- [17] Andreas Mielke. The hubbard model and its properties. In Eva Pavarini, Piers Coleman, and Erik Koch, editors, *Many-Body Physics: From Kondo to Hubbard*, volume 5 of *Modeling and Simulation*, 2015.
- [18] Holger B Nielsen and Masao Ninomiya. Dirac sea for bosons i: Formulation of negative energy sea for bosons. *Progress of Theoretical Physics*, 113(3):603–624, 2005.
- [19] Silvia Noschese, Lionello Pasquini, and Lothar Reichel. Tridiagonal toeplitz matrices: Properties and novel applications. *Numerical Linear Algebra with Applications*, 20(2):302–326, 2013.
- [20] Frank WJ Olver, Daniel W Lozier, Ronald F Boisvert, and Charles W Clark. *NIST Handbook of Mathematical Functions*. Cambridge University Press, 2010.
- [21] M.E. Peskin and D.V. Schroeder. *An Introduction to Quantum Field Theory*. Perseus Books, 1995.
- [22] David Raventós, Tobias Graß, Maciej Lewenstein, and Bruno Juliá-Díaz. Cold bosons in optical lattices: a tutorial for exact diagonalization. *Journal of Physics B: Atomic, Molecular and Optical Physics*, 50(11), 2017.
- [23] Jun John Sakurai and San Fu Tuan. *Modern Quantum Mechanics*. Addison Wesley, revised edition edition, 1995.
- [24] Richard T. Scalettar. An introduction to the hubbard hamiltonian. In Eva Pavarini, Erik Koch, Jeroen van den Brink, and George Sawatzky, editors, *Quantum Materials: Experiments and Theory*, volume 6 of *Modeling and Simulation*, 2016.
- [25] Daniel V Schroeder. *An Introduction to Thermal Physics*. Addison Wesley, 1999.
- [26] Jacob F Sherson, Christof Weitenberg, Manuel Endres, Marc Cheneau, Immanuel Bloch, and Stefan Kuhr. Single-atom-resolved fluorescence imaging of an atomic mott insulator. *Nature*, 467(7311), 2010.
- [27] Christof Weitenberg. *Single-Atom Resolved Imaging and Manipulation in an Atomic Mott Insulator*. PhD thesis, LMU Munich, 2011.
- [28] Sebastian Will. *Interacting Bosons and Fermions in Three-Dimensional Optical Lattice Potentials*. PhD thesis, Johannes Gutenberg-Universität Mainz, 2011.
- [29] J.M. Zhang and R.X. Dong. Exact diagonalization: the bose–hubbard model as an example. *European Journal of Physics*, 31(3), 2010.